SYNTHESIS AND CHARACTERIZATION OF NIOBIUM PENTOXIDE THIN FILMS PREPARED BY SPRAY PYROLYSIS TECHNIQUE FOR DYE SENSITIZED SOLAR CELL APPLICATION

KINEENE MIRIAM MWONGELI (B.Ed TECH)

I56/23514/2011

A Thesis Submitted in Partial Fulfillment of the Requirements for the Award of the Degree of Master of Science (Electronics and Instrumentation) in the School of Pure and Applied Sciences of Kenyatta University

March 2019

DECLARATION

This work is my own original work and has not been presented for the award of degree or for any other awards in any other university.

Signature…….. Date…….……

Miriam M. Kineene
Department of Physics

SUPERVISORS

We confirm that the work reported in this thesis was carried out by the candidate under our supervision.

Signature…….. Date…….……

Dr. Mathew K. Munji
Department of Physics
Kenyatta University

Signature…….. Date…….……

Prof. Justus Simiyu
Department of Physics
Masai Mara University

DEDICATION

This thesis is dedicated to my dear husband Eng. Benjamin Mutua and our lovely sons Stephen Amani and Victor Mumo.

ACKNOWLEDGEMENTS

I thank the almighty God for His blessings and for directing my paths; through His guidance I have completed my research successfully. Blessed be His holy name. I thank my supervisors Dr. Mathew Munji (Kenyatta University) and Prof. Justus Simiyu (Masai Mara University) for their advice, guidance, support, patience and understanding during this research work, God bless you richly.

I am grateful to the Vice Chancellor of Kenyatta University Professor Paul Wainaina for providing a favourable learning environment. I acknowledge the staff members of the Physics department, Kenyatta University led by Dr. Nadir Hashim for their support during the research period.

Special thanks to Mr. Muthoka Benson of Solid-State Laboratories, University of Nairobi (Chiromo campus) for his guidance on how to use machines and also for introducing to me Mr. Godwin Asiimwe who supported in carrying out tests in the laboratory.

I acknowledge the national commission for science and technology (NACOSTI) for financial support in acquiring chemicals and materials used in this work.

Finally and most importantly, I thank my dear husband Eng. Benjamin Mutua for his financial support, words of encouragement and his patience, understanding and moral support during my course. God bless you.

TABLE OF CONTENTS

DECLARATION ii
DEDICATION iii
ACKNOWLEDGEMENTS iv
TABLE OF CONTENTS v
LIST OF FIGURES viii
LIST OF TABLES x
ABBREVIATIONS AND ACRONYMS xi
ABSTRACT xiii

CHAPTER ONE
INTRODUCTION

1.1 Background information 1
1.2 Solar PV technology generations 3
1.2.1 First generation solar PV 3
1.2.1.1 Mono crystalline silicon solar cells 3
1.2.1.2 Polycrystalline silicon solar cells 4
1.2.2 Second generation PV - Thin film solar PV 4
1.2.2.1 Amorphous silicon thin film (a-Si) solar cell 5
1.2.2.2 CdTe solar cells 5
1.2.2.3 Copper Indium Gallium Di-Selenide (CIGS) solar cells 6
1.2.2.4 Gallium Arsenide solar cells (GaAs) 8
1.2.3 Third generation solar PV 9
1.2.3.1 Polymer solar cells 9
1.2.3.2 Nano-crystal based solar cells 9
1.3 Statement of the problem 12
1.4 Objectives 13
1.4.1 General objective 13
1.4.2 Specific objectives 13
1.5 Rationale of the study 14

CHAPTER TWO

LITERATURE REVIEW

2.1 Overview of Niobium Oxide 15
2.2 Operation Principle of Dye Sensitized Solar Cell 16
2.3 Related Studies 17

CHAPTER THREE

THEORETICAL BACKGROUND

3.1 Introduction 20
3.1.1 Crystal Structure of Niobium Pentoxide 21
3.2 Deposition Methods for Niobium Pentoxide Thin Films 22
3.2.1 Liquid Phase Deposition Methods 22
3.2.2 Solvo-thermal Methods 22
3.2.3 Anodization Technique 23
3.2.4 Sol-gel Method 24
3.2.5 Electro-deposition 24
3.3 Vapor Phase Deposition 25
3.3.1 Physical Vapor Deposition (PVD) 25
3.3.2 Chemical Vapor Deposition (CVD) 26
3.3.3 Spray Pyrolysis Deposition Technique 26
3.4 Optical Reflectance 27
3.5 Optical Transmittance 28
3.6 Semiconductor and Energy Bands 28
3.6.1 Direct and Indirect Band Gap 30
3.7 The Absorption Coefficient 31
3.8 XRD Structural Analysis 32

CHAPTER FOUR

MATERIALS AND EXPERIMENTAL PROCEDURES

4.1 Introduction 34
4.2 Cleaning of the Substrate 34
4.3 Preparation of Precursor Solution 35
4.4 Preparation of the Films 35

4.5 Characterization 38
4.5.1 Optical Characterization 38
4.5.2 Estimation of energy band gap 40
4.6 Sheet Resistivity 41
4.7 XRD Characterization 43

CHAPTER FIVE

RESULTS AND DISCUSSION

5.1 Optical Spectra of Thin Films 45
5.2.1 Effect of spray duration on transmittance and reflectance of niobium pentoxide thin films 45
5.2.2 Effect of temperature on transmittance and reflectance 50
5.2.3 Effect of spray duration and temperature on the thickness of Nb_2O_5 thin films 51
5.3 Absorption coefficient. 52
5.3.1 Energy band gap 53
5.4 Electrical properties 55
5.5 Structural Characteristics 56

CHAPTER SIX

CONCLUSIONS AND RECOMMENDATIONS

6.1 Conclusions 60
6.2 Recommendations 61
6.2.1Recommendation for future studies 62
REFERENCES 63
APPENDIXES 68

LIST OF FIGURES

Figure 1.1: Schematic diagram showing the working of a solar cell……2

Figure 1.2: Layers of a CdTe solar cell……6

Figure 1.3: Layers of a CIGS solar cell ……7

Figure 1.4: Cross-section of GaAs solar cell……8

Figure 1.5: Single junction dye sensitized solar cell……11

Figure 2.1: Operation principle of DSSC……16

Figure 3.1: Energy diagram of a semiconductor……29

Figure 3.2: Energy band diagram of a semiconductor……31

Figure 3.3: Bragg reflections from a particular family of lattice planes……33

Figure 4.1: Sonicater machine……35

Figure 4.2: Automated spray pyrolysis equipment……37

Figure 4.3: Scheme of the spray pyrolysis setup……38

Figure 4.4: DUV 3700 solid spectrophotometer……39

Figure 4.5: $(\alpha hv)^2$ versus photon energy (hv) for Nb_2O_5 thin film……41

Figure 4.6: Schematic diagram of four point probe configuration……42

Figure 4.7: Determination of FWHM of Nb_2O_5 thin film……44

Figure 5.1: (a) Transmittance of Nb_2O_5 thin films sprayed at a temperature of 270^oC……46

Figure 5.1: (b) Reflectance of Nb_2O_5 thin films sprayed at a temperature of 270^oC……46

Figure 5.2: (a) Transmittance of Nb_2O_5 thin films sprayed at a temperature of 370^oC……47

Figure 5.2: (b) Reflectance of Nb_2O_5 thin films sprayed at a temperature of 370^oC……48

Figure 5.3: (a) Transmittance of Nb_2O_5 thin films sprayed at a temperature of 470^oC……...……..……49

Figure 5.3: (b) Reflectance of Nb_2O_5 thin films sprayed at a temperature of 470^oC……...…….……49

Figure 5.4: (a) Transmittance of Nb_2O_5 thin films sprayed at duration of two minutes……...…..……50

Figure 5.4: (b) Reflectance of Nb_2O_5 thin films sprayed at duration two minutes……...…...……51

Figure 5.5: $(\alpha h\nu)^2$ versus photon energy curve for Nb_2O_5 thin film deposited at 470^oC at a spray duration of two minutes.....…….…… 53

Figure 5.6**:** X-ray Diffraction pattern of Nb_2O_5 thin films deposited at 270^oC, 370^oC and 470^oC at a spray duration of two minutes……...……....57

Figure 5.7: X-ray Diffraction patterns of Nb_2O_5 thin films deposited at 1 min, 2 min and 3 min at a substrate temperature of 470 ^oC…..…..……...…58

Figure 5.8: Diffraction broadening of Nb_2O_5 thin film at 12.39^o …….....……59

LIST OF TABLES

Table 3.1: Properties of different Nb_2O_5 crystal phases……...……..…22

Table 4.1: Preparation of precursor solution……...…….……...…..….36

Table 5.1: Variation of thickness of Nb_2O_5 thin films with duration ……...….52

Table 5.2: Variation of thickness of Nb_2O_5 thin films with temperature..…….52

Table 5.3: Band gap values for Nb_2O_5 thin film sprayed at different substrate temperatures and different durations ……..……54

Table 5.4: Variation of sheet resistance of Nb_2O_5 thin films with temperature...……..……...……..55

Table 5.5: Variation of sheet resistance of Nb_2O_5 thin films with duration……...56

Table 5.6: Crystal size derived from FWHM at the orientation of 220 plane..….....59

ABBREVIATIONS AND ACRONYMS

APCVD	Atmospheric pressure chemical vapour deposition
A-Si	Amorphous silicon
CIGS	Copper indium gallium diselenide
CdTe	Cadmium telluride
COD	Crystallography Open Database
CVD	Chemical vapour deposition
DC	Direct current
DSSC	Dye Sensitized Solar Cells
FWHM	Full Width at Half Maximum
GaAs	Gallium arsenide
H_2O	Water
H_2O_2	Hydrogen peroxide
InGaP	Indium gallium phosphide
ITO	Indium-doped Tin Oxide
$KNbO_3$	Potassium Niobate Crystal
$LiNbO_3$	Lithium Niobate Crystal
MOCVD	Metal organic chemical vapour deposition
Nb	Niobium
Nb_2O_3	Niobium Trioxide

Nb_2O_5	Niobium Pentoxide
Nb $(OC_2H_5)_5$	Pentaethoxy niobium
$NbCl_5$	Niobium pentachloride
NbO	Niobium Oxide
O_2	Oxygen
PECVD	Plasma-enhanced chemical vapour deposition
PLD	Pulsed laser deposition
PSC	Polymer Solar Cells
PUMA	Point wise unconstrained minimization approach
PV	Photovoltaic
PVD	Physical vapour deposition
QD	Quantum dots
RF	Radio Frequency
SnO_2	Tin dioxide
TiO	Titanium Oxide
VLS	Vapour-liquid-solid
XRD	X-ray Diffraction
ZnO	Zinc oxide

ABSTRACT

There is a rapid increase in demand for energy worldwide and one of the most promising approaches to resolve this crisis is through use of photovoltaic technologies. Dye sensitized solar cells (DSSC) are attractive candidates in this regard. This is because the materials they use are of low cost and non-toxic. Niobium pentoxide (Nb_2O_5) thin films have been stable as photo anode for DSSC. Methods that are used to deposit niobium pentoxide thin films include hydrothermal method, solgel method, anodization technique, electro-deposition, sputtering, and spray pyrolysis. Among the above mentioned methods, spray pyrolysis is the simplest. It is a low cost method especially with regard to equipment. The technique requires chemicals that can undergo pyrolysis. In this study, Niobium pentoxide (Nb_2O_5) thin films for DSSC application were deposited on ordinary glass substrates using the spray pyrolysis technique. In the synthesis of Nb_2O_5, Niobium pentachloride ($NbCl_5$) was used a precursor solution. This was prepared by dissolving Niobium pentachloride in distilled water to which hydrogen peroxide and acetic acid were added. The deposition parameters of the niobium thin films such as spray duration and substrate temperature were varied. The sprayed solution underwent thermal decomposition resulting in formation of niobium pentoxide (Nb_2O_5) thin films. The optical characteristics of the films were determined using the Shimadzu model DUV 3700 spectrophotometer. From the transmittance spectra obtained, it was clear that the films were 60% to 90% transparent in the visible region and the absorption edge occurred at around 300nm. Sheet resistivity of the films determined by use of the four point probe method was $10^{-4}\Omega$cm. XRD studies revealed that the films were tetragonal in nature with well defined reflections at (211) and (220). The average crystallite size was estimated to be 21.25nm. The thicknesses of the films were determined using the KLA Tencor Alpha–step IQ surface profiler and was found to range between 162nm and 517nm. Band gap energy and absorption coefficient were estimated using point-wise unconstrained minimization approach (PUMA) software. Band gap energy values ranged between 3.92 eV to 4.12 eV. From the obtained results, the films considered best for DSSC application were those deposited at substrate temperature of 470^oC and at duration of 2 minutes.

CHAPTER ONE

INTRODUCTION

1.1 Background information

The worldwide energy demand is rapidly increasing, coupled with diminishing fossil fuels resources and their associated climate change effects. Therefore, there is an urgent need for sustainable energy technologies that are environmentally friendly. Among them, the renewable energy technologies such as hydropower, wind, wave and tidal energy, biomass, solar thermal, solar photovoltaic (PV), derived liquid fuels and biomass fired electricity generation; PV technology is most readily deployable (Basiru and Muhamed, 2012).

Solar energy refers to the tremendous amounts of energy sent out by the sun in form of sunlight and heat. It is a renewable source of energy which does not pollute the environment, free from noise and a cost free resource. There are two major solar energy conversion technologies; the first one is the thermal conversion technology which is further categorized into heating and electrical power production. Black surfaces exposed to beams of sunlight absorb the solar energy and change it into heat which is utilized in heating systems. By combining difference in air pressure and green house effect, air currents produced are used to rotate blades of turbine to generate electrical energy from sunlight. Rays of the sun can also be concentrated over a small area by use of reflectors and thus its heat can be used in raising steam. This steam is used to drive steam turbine that is coupled to alternator to produce electricity (Mukrimin, 2016). The second solar energy conversion technology is photovoltaic (PV) technology. This involves use of photovoltaic cells that harvest sunlight and converts it into electricity.

PV cells contain semiconductor materials whose conducting properties can be altered by adding impurities in a controlled manner into the pure semiconductor. If the semiconductor has excess electrons, it is referred as n-type semiconductor and if it has holes (lack of electrons) it is known as p-type semiconductor. When n-type semiconductor is suitably joined with p-type and light shines on them, electrons can flow from n-type to p-type and this effect is called photovoltaic effect (Çakanyıldırım, 2017).

There are three factors which govern the working mechanism of photovoltaic cells: first the absorption of light causing generation of charge careers, i.e. electrons and holes. Secondly charge carrier separation takes place and finally the charge carriers produced are collected at their respective electrodes; - This enhances the creation of a potential difference across the pn junctions. When visible light falls on the pn junction, voltage realized in it is utilized in doing work (Sharma *et al.*, 2015). Figure 1.1 is a schematic diagram showing the working of a solar cell.

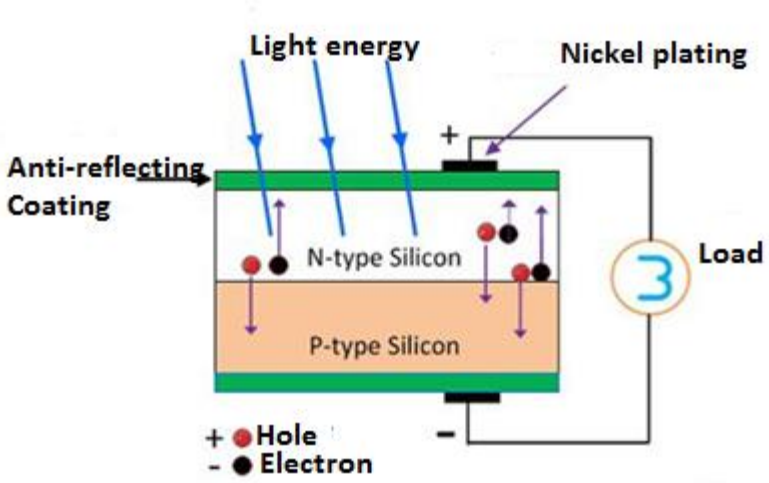

Figure 1.1: Schematic diagram showing the working of a solar cell (Circuit globe, 2019).

1.2 Solar PV technology generations

1.2.1 First generation solar PV

The first generation solar PVs are manufactured from silicon wafers. Silicon wafer technology is the oldest and also forms the largest number of the widely commercialized solar cells because of high power efficiencies obtained. In addition, silicon is usually extracted from sand and quartz which are readily available in nature (Bharam, 2012). First generation solar PVs are of two types, i.e. monocrystalline solar cells and polycrystalline solar cells (Choubey *et al.*, 2012).

1.2.1.1 Mono crystalline silicon solar cells

The other name for monocrystalline solar cells is single crystalline solar cells. They normally have uniformity in their external coloring which is an indication of high purity and therefore easy to recognize them. Such cells are made up of silicon of highest grade which makes them have the highest efficiency. Single crystalline solar panels have power efficiency that ranges between 15 to 20%. They have longer life and in terms of performance under conditions of low light, they are better than solar cells made of polycrystalline silicon (Mathias, 2013).

Nevertheless the single crystalline solar cells are mainly expensive due to the Czochralski process employed in the production of high grade monocrystalline silicon. It involves the melting of high grade silicon in a crucible at a temperature of 1425^{o}C. In order to dope the molten silicon, impurities such as boron and phosphorus are added in succession. The next steps consist of dipping a rod-mounted seed crystal into the molten silicon. The seed crystal has a well-defined crystal orientation. Next, the crystal's rod is cautiously pulled out and it is simultaneously rotated. The temperature

gradients, speed of rotation, and the rate of pulling must be precisely controlled. Such process results in the production of huge cylindrical ingots from the molten silicon which is cut to make silicon wafers. This results into waste of a considerable amount of the original silicon. The melting process is very slow and requires huge amount of energy that increases the production cost (Thomas, 2018).

1.2.1.2 Polycrystalline silicon solar cells

Polycrystalline solar cells are also referred to as multicrystalline. This technology has gained popularity because of high power efficiencies. Solar cells made of polycrystalline silicon do not require the Czochralski process. Different crystals connected together in single cell form a PV module. In manufacture of such solar cells, raw silicon is melted and then poured into square mold after which it's sliced perfectly in to square wafers. These cells have less heat tolerance than single crystalline solar cells and hence in high temperatures, they perform slightly worse than single crystalline solar panels. The efficiency of solar panels made from polycrystalline silicon is typically 11-14%. During the year 2008, they were considered to constitute up to 48%, in terms of solar cells manufacturing worldwide (Saga, 2010).

1.2.2 Second generation PV - Thin film solar PV

The second generation PV constitutes the thin film technology. Such photovoltaic are classified according to the type of photovoltaic material that is deposited on the substrate. They include amorphous silicon (a-Si), cadmium telluride (CdTe), copper indium gallium diselenide (CIGS) and gallium arsenide (GaAs).

1.2.2.1 Amorphous silicon thin film (a-Si) solar cell

Amorphous silicon solar cells require much less silicon as compared to monocrystalline and polycrystalline solar cells. The substrates used can be made out of materials of low cost such as stainless steel, glass, and plastic. This means that they have an advantage of being relatively cheaper as compared to monocrystalline and polycrystalline solar cells which makes them readily available. In solar cells the word “amorphous” means that the silicon material which comprises the solar cell do not have definite pattern or structure which is a characteristic in crystalline materials. The atoms in the lattice lack specific arrangement that makes it to be non-crystalline. To fabricate solar cells using thin films made of amorphous silicon, doped silicon material is mainly used to coat the backside of the substrate (or glass plate). Generally, the color on the reflecting side of a-Si is dark brown while the color on the conducting side is silverfish (Grein Energy, 2015).

Instability and poor efficiency is the major disadvantage of a-Si solar cell. The current PV modules efficiency is quite low. It ranges between 4% and 8 % (Maehlum, 2015).

1.2.2.2 CdTe solar cells

Cadmium telluride (CdTe) happens to be the predominant thin film technology. It forms around 5% of the world’s solar cell production (Solar energy technologies office, 2017). With this technology, it is possible to produce cheaper photovoltaic devices. The band gap of CdTe is 1.5 eV. It has high optical absorption coefficient and it is chemically stable (Sharma *et al.,* 2015). These properties make CdTe an

attractive material for the manufacturing of thin film solar cells. CdTe is a crystalline compound semiconductor which has an excellent direct band gap. This is a clear indication that light is absorbed with a lot of ease and also the solar cell efficiency is improved. Figure 1.2 shows the layers of a CdTe solar cell.

Majorly, CdTe solar cells comprise of a p-n heterojunction structure that contains a layer of p-doped CdTe that is matched with a layer of n-doped cadmium sulfide (CdS). This layer acts as the window layer. The efficiency of CdTe solar cells ranges between 9% and 11 % (Badawy, 2015).

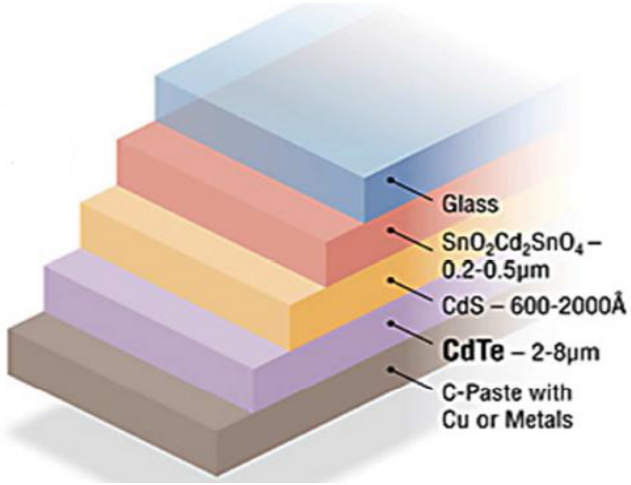

Figure 1.2: Layers of a CdTe solar cell (Bagher *et al.,* 2015).

1.2.2.3 Copper Indium Gallium Di-Selenide (CIGS) solar cells

CIGS is a compound semiconductor that comprises of the following elements: Copper, Gallium, Indium, and Selenium. The band gap type in CIGS semiconductor is direct. CIGS solar cell has higher efficiencies (10% - 12%) as compared to CdTe (Sharma *et al.,* 2015). CIGS is one of the most promising thin film technologies due

to its economy and high efficiency. Methods such as evaporation, sputtering, printing, electron beam deposition and electrochemical coating are employed in the processing of CIGS solar cells (Srinivas *et al.*, 2015). The substrates for depositing CIGS solar cells can be selected from materials such as glass plate, steel, polymers substrates among others. Figure 1.3 is graphic representation of CIGS solar cell layers.

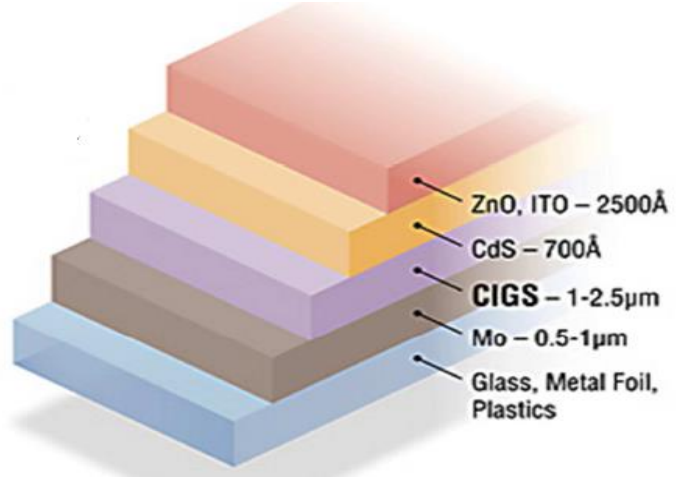

Figure 1.3: Layers of a CIGS solar cell (Bagher *et al.*, 2015).

The main drawback is that CIGS and CdTe contain the toxic material cadmium. It is a potential carcinogen which can accumulate in the tissues of both plants and animals. A smaller amount of cadmium is contained in CIGS solar cells as compared to cadmium telluride solar cells. In some situations especially in high temperatures where multi kilowatt systems are involved, solar panels made of CdTe can be cheaper as compared to those made of monocrystalline and polycrystalline silicon. Thin film solar cells have lower efficiency rates as compared to crystalline solar cells and tend to degrade faster (Maehlum, 2013). Cd based materials are poisonous and this implies that their disposal and also the process of recycling them can be

costly and a harmful to the environment (Bagher *et al.*, 2015). Hence, restricted supply of cadmium together with hazards that it poses to the environment, are the major challenges facing these types of solar cells (Antonio, 2003)

1.2.2.4 Gallium Arsenide solar cells (GaAs)

GaAs consists of two elements; gallium and arsenic. It is a semiconductor with high electron mobility than silicon. In fabrication of GaAs solar cells, a window layer of InGap is used. Due to the difference in refractive index between InGap and air, a considerable amount of light can be reflected from the solar surface. This necessitates use of antireflection layer in order to improve the light conversion efficiency. The disadvantage with GaAs solar cell is the high production cost of the single crystal. In addition, gallium is a rare metal and arsenic is poisonous (Kanghao *et al.*, 2013). Figure 1.4 shows the cross-sectional structure of a GaAs solar cell.

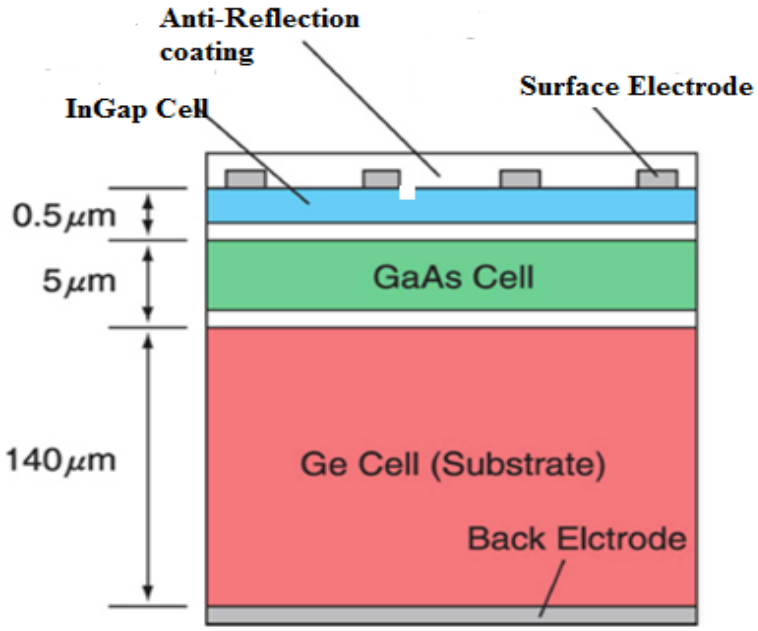

Figure 1.4: Cross-section of GaAs solar cell.

1.2.3 Third generation solar PV

Although the third generation solar PV are the latest promising technologies, they haven't been commercially explored in detail. Some of the developed third generation solar photovoltaics are

1) Polymer solar cells.

2) Dye sensitized solar cells.

3) Nano crystal based solar cells.

1.2.3.1 Polymer solar cells

In general, Polymer solar cells (PSC) are flexible because of the polymer substrate. A PSC is composed of thin functional layers coated on a polymer ribbon or foil that is connected in series. Its working mechanism is mainly as a combination of donor (polymer) and an acceptor (fullerene). A variety of materials such as organic form of conjugate/conducting polymer are used for sunlight absorption (Ganesh *et al.*, 2013).

1.2.3.2 Nano-crystal based solar cells

The other name for nano-crystal based solar cells is Quantum dots (QD) solar cells. They are generally made of a semiconductor belonging to the transition metal groups. Their sizes are in the nano-crystal range made from the semiconductor. QD is a name used to refer to crystal size that ranges within a few nanometers; some examples include materials such as porous TiO_2 or porous Si, which are often used in Quantum dot solar cells (Hoppe and Sariciftci, 2008).

1.2.3.3 Dye Sensitized Solar Cells (DSSC)

DSSC is a photo- electrochemical system that employs organic materials. The DSSC comprises of; photo anode which is made up of mainly titanium dioxide nanoparticles, a platinum contact that acts as the counter electrode, and a dye sensitizer and redox mediator. The dye sensitizer is the photoactive component and it acts as the electron donor. The advantage with such cells is that they are highly flexible and are inexpensive due to simple processing techniques employed in their manufacture. The novelty in the dye sensitized solar cells is as a result of the photosensitization which occurs at the surface of TiO_2 nanoparticles that are covered with optically active dye that is visible. This increases the efficiency to values greater than 10 % (Li *et al.*, 2006).

Among the various types of solar cells discussed above, the most widely commercialized solar cells currently are the silicon based mainly monocrystalline silicon and polycrystalline silicon. They are made out of highest grade silicon and the manufacturing process employed is expensive and therefore a cheaper alternative to silicon solar cells is the dye sensitized solar cell. DSSC consist of a wide gap semiconductor formed between anode that is sensitized with visible light absorbing species (dye), an electrolyte and a photoelectrical system (Essner, 2011). The band position of the metal oxide semiconductor is relative to that of the sensitizer. The nanoporous metal oxides offer high surface area that facilitates the improvement in absorption of light and also improved loading of the dye for better performance of DSSC. Metal oxides used for fabrication of dye sensitized solar cells have solar absorption below threshold wavelength which is given by equation 1.1

$$\lambda_g = \frac{1240}{E_g} \tag{1.1}$$

where λ is the wavelength in nm and E_g is band gap of the metal oxide. So light in the visible and near infrared region is absorbed by the dye. The strong absorption of light is due to the intramolecular charge transfer transition from the donating to the anchoring acceptor group of the dye. Hence, the anchored dye on the metal oxide surface aids the red shift of the absorption threshold of metal oxide near infrared region. Besides the above physical qualities, the inexpensiveness, natural abundance and facile synthesis techniques of metal oxides and their composites is an added advantage of their application in DSSC (Lee *et al.*, 2011). The DSSC could become a potential alternative for the traditional silicon and thin film panels in the near future (Toivola, 2010). Figure 1.1 shows the cross-section construction of DSSC solar cell.

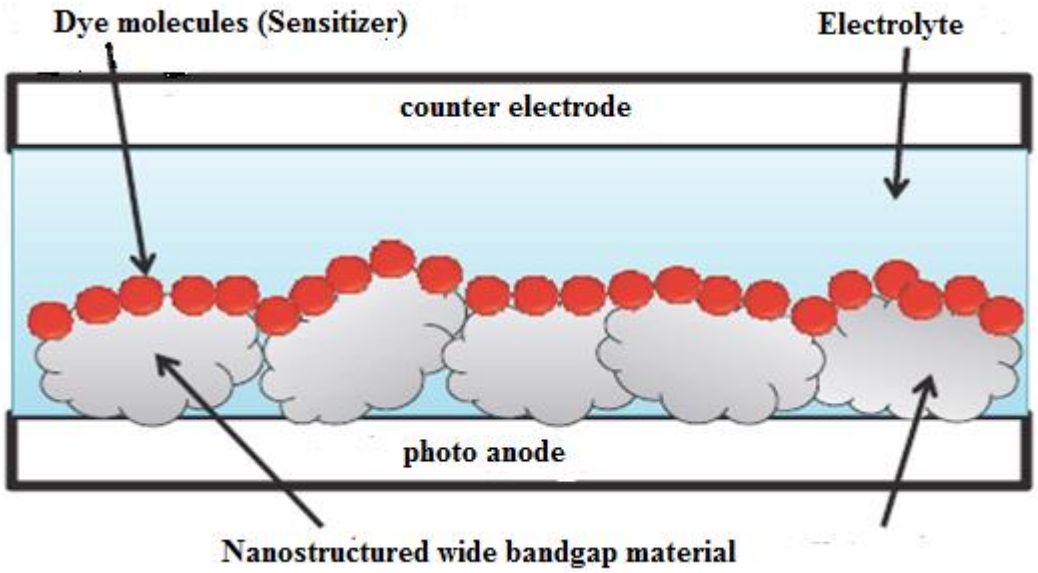

Figure 1.5: Single junction dye sensitized solar cell (Jasim, 2011

The photo anode and counter electrode are coated with thin conductive and transparent film such as fluorine doped tin dioxide. The type of substrate commonly used is clear glass. This is because of their optical transparency in the visible and near infrared regions of the electromagnetic spectrum. In addition, glass substrates are readily available at low costs. Thin transparent conducting oxide is deposited on one side of the glass substrate to form a conductive coating/film. The conductive coating ensures that the resistance per square is very low. The typical value for resistance per square at room temperature ranges between 10 ohms and 20 ohms. The nanostructure wide gap oxide is grown on the conductive side of the substrate. Before the cell is assembled, the counter electrode should be coated with a layer of catalyst such as graphite in order to facilitate the mechanism of donating electrons to the electrolyte (Jasim, 2011).

In DSSC, light is absorbed by the anchored dye and charge separation takes place at the interface via photo induced electron injection from the dye on to the conduction band of the semiconductor (Wang *et al.*, 2006). In this study, spray pyrolysis was used in the production of nanocrystalline and porous Nb_2O_5 thin films as photo anode for DSSC application.

1.3 Statement of the problem

Single p-n junction silicon based solar cells are the most popular type of solar cells that are used widely for commercial purposes. Silicon solar cells have an advantage of high efficiencies but the disadvantage is that to attain such performance, materials of high purity are used. In addition expensive fabrication methods have to be employed. Dye sensitized solar cell (DSSC) is a cheaper alternative to silicon based

solar cells. Nb_2O_5 thin films have been stable in DSSC application. Techniques used to deposit Nb_2O_5 thin films include sputtering, spray pyrolysis, electrodeposition, anodization, sol-gel methods, and hydrothermal methods. Among the above listed methods, spray pyrolysis presents a simple method. However this technique has not been fully exploited despite the fact that it's a relatively cheap techique that could be scaled up for mass production. The major challege with spray pyrolysis is the optimization of the deposition parameters such as precursor solution concetration, substrate temperature, carrier gas pressure, spray duration and nozzle-substrate distance.

1.4 Objectives

1.4.1 General objective

To characterize niobium pentoxide thin films prepared by spray pyrolysis technique for dye sensitized solar cell application.

1.4.2 Specific objectives

(i) To Deposit Nb_2O_5 onto glass substrates using spray pyrolysis technique under various substrate temperatures and spray durations.

(ii) To investigate the optical characteristics of the as prepared Nb_2O_5 thin films.

(iii) To investigate the electrical characteristics of the as prepared Nb_2O_5 thin films.

(iv) To analyze the structural characteristics of Nb_2O_5 thin films using XRD.

1.5 Rationale of the study

The demand for electrical energy has greatly risen. The development of clean renewable energy sources to satisfy the rise in energy demand by our society has become one of the most important global issues to be solved in this country. Energy generation from solar radiation using photovoltaic technology is considered as one of the remedies for this worldwide issue. This has necessitated the research in new materials for solar cell application which forms a reliable alternate source of electrical energy generation.

The most common commercially available solar cells are the single crystalline and multicrystalline. These solar cells are expensive and require pure materials in their manufacture using a lot of energy in their purification. An alternative to these are the DSSC which are easy to fabricate and uses materials of low cost.

CHAPTER TWO

LITERATURE REVIEW

2.1 Overview of Niobium Oxide

Stochiometric niobium oxides exist mainly in the following forms of Nb_2O_5, Nb_2O_3 and NbO. The most widely studied material is niobium pentoxide (Nb_2O_5) (Aegerter *et al.,* 2002). Methods that have been employed in the preparation of niobium pentoxide include oxidizing niobium metal in air, hydrolysis of metallic niobiates, niobium pentachloride and niobium alkoxides. It can also be obtained by precipitation from solution in hydrofluoric acid with alkali metal hydroxide or ammonia. Traditionally niobium pentoxide is used in metallurgy for producing hard materials or as an additive in optics to prevent the devitrification and to control the refractive index of special glass. It is used in electronics for the preparation of electro-acoustic or electro-optical components such as $KNbO_3$ and $LiNbO_3$.

In the last fifteen years, the interesting conducting properties of Nb_2O_5 together with the initiation of more advanced preparation techniques and systems that can be controlled, it has been possible to obtain extremely fine powders, highly porous materials, and coatings. Such materials have found further important application in the field of batteries electrochromism, catalysis, and solar cells (Aegerter *et al*., 2002). Nb_2O_5 is resistant to corrosion in both acidic and base media and has excellent chemical stability (Mujawar *et al*., 2006).

Nanocrystalline dye sensitized solar cells (DSSC) using niobium thin films have been reported. The properties of the films relied on deposition method or technique, the deposition parameters, the sputtered material, film thickness among other

factors. The deposition methods being used to prepare niobium pentoxide films include anodic deposition, thermal oxidation, vacuum evaporation, sputtering, sol-gel, spray pyrolysis and spin coating (Kovendhan *et al*., 2011).

Among the physical and chemical methods mentioned above, spray pyrolysis is the simplest. It's a low cost method especially in terms of the equipment used. It also presents a very simple technique for depositing films of any composition. Substrates and chemicals required are not of high cost (Perednis and Gauckler, 2005).

2.2 Operation Principle of Dye Sensitized Solar Cell

Figure 2.1 is schematic diagram of the operating principle of a TiO_2 based DSSC

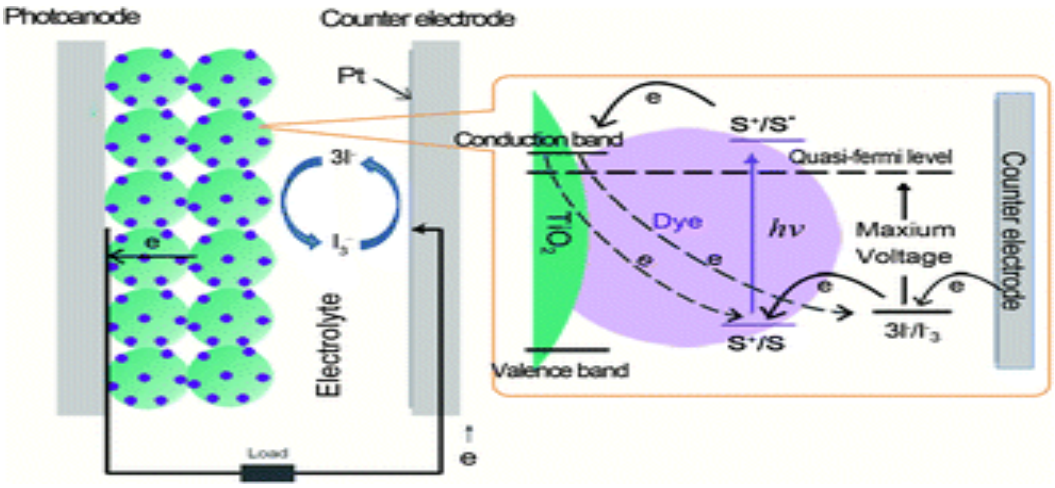

Figure 2.1: Operation principle of DSSC (Hong-yan *et al*., 2012)

When light shines on DSSC, it is absorbed by the dye molecules adsorbed on TiO_2 surface. The dye molecules in turn create excitation pairs (S*) which rapidly split on the TiO_2 surface. The excited electrons are injected into the conduction band of TiO_2 electrode resulting into oxidation of the dye molecule (S^+). The electrons then diffuse to the back contact of the photoanode and are subsequently transported to the

counter electrode via an external circuit in miliseconds. The oxidised dye molecule (S^+) is reduced by the iodine redox mediater (I^-/I^{3-}) and as a result it is regenerated to ground state (S). The oxidised redox mediator (I^{3-}) diffuses to the counter electrode where it is recovered. Hence a closed circuit is thereby set up to continously convert the solar energy into electrical energy.

2.3 Related Studies

Kovendhan *et al.* (2011) deposited niobium pentoxide thin films by spray pyrolysis on ITO substrates with the aim of testing the suitability of spray deposited niobium pentoxide thin films for application in electrochromism and solar cells. XRD analysis revealed tetragonal phase of the films. Transmittance spectra showed the film to have high transparency in the visible region. However, they did not report the electrical properties of the prepared films.

Patil *et al.* (2005) investigated the effect of substrate temperature and post annealing temperature on the structural, optical and electrical properties of Nb_2O_5 thin films. They observed that with increase in temperature, films turned more polycrystalline. Also from their findings, annealed films exhibit higher crystallinity and became more transparent. Parameters like film thickness, band gap energy and electrical resistivity decrease as temperature is increased. However the band gap obtained was too low while electrical resistivity reported was too high. Moreover, precursor preparation involved the use of many chemicals.

Perednis and Gauckler (2005) conducted a comprehensive review on thin films deposited by spray pyrolysis. From the various researches conducted, it was clear

that with increase in spray temperature, the film morphology changed from a cracked to a porous microstructure. It was also reported that with high temperatures the films became more rough and porous. Change in the composition of the precursor solution can be used to tailor the structure and properties of the deposited film. The morphology of the films can be changed considerably by applying additives to the precursor solution. For instance TiO_2 thin film structure changed from cracked to crack free reticular after introducing acetic acid in to the precursor solution chemistry.

Naofumi *et al*. (2003) prepared niobium oxide nanoparticles by peroxo niobic acid obtained by peptization of niobic acid precipitate with hydrogen peroxide aqueous sol. From this study, XRD patterns formed were much influenced by the concentration of niobic acid precipitate used. Crystallinity was also seen to increase with increase in temperature.

Amita and Singh (2013) prepared nanocrystalline Nb_2O_5 films by sol-gel spin coating process. From their results the existence of Nb_2O_5 crystallites in the film was confirmed from the appearance of distinct diffraction peaks. The crystal structure of Nb_2O_5 crystallites were identified as hexagonal. A color change from transparent to blue was observed for niobium oxide film upon application of electric field to its crystallite behavior. The films were found to exhibit high transmittance and low reflectance in the visible spectra. However, the method used is time consuming and it’s also difficult to control the porosity of the films. Moreover, bonding inside the film prepared by sol-gel is usually weak and this necessitates heat treatment. It can be concluded that despite Nb_2O_5 being a promising metal oxide semiconductor for

photovoltaic cells, it has not yet been fully explored. This study varied deposition parameters, where Nb_2O_5 thin films were prepared and characterized for DSSC application.

CHAPTER THREE

THEORETICAL BACKGROUND

3.1 Introduction

Although Niobium pentoxide is a metal oxide with great potential, it has not been fully exploited up to date. The existence of various forms of Nb_2O_5 was first studied in the early 1940s. It has a chain of interesting structural phases. Nb_2O_5 phases depend upon NbO_6 octahedral groups, it forms a wide range of arrangements from the rectangular blocks. **N**iobium pentoxide is readily available in nature, highly resistive to corrosion and it is thermodynamically stable (Michael *et al.,* 2014).

In the initial stages of research on Nb_2O_5, the material was mostly studied in thin layer forms or in bulk and also in suspensions (Sanchez *et al.,* 1991). The very first applications of Nb_2O_5 were investigated as sensors, catalysts and as an electrochromic material. In such studies, the distinctive performance of Nb_2O_5 was due to the identification of crystal phases and understanding of its energy band diagram, which created curiosity among researchers to investigate further on the metal oxide's capabilities. Currently, Nb_2O_5 has become very popular, different researchers have reported a variety of Nb_2O_5 which range from large crystals and bulk crystals to various nanostructures (Rani *et al*., 2014). In particular, nanostructured Nb_2O_5 normally has high surface area to volume ratio. In addition, the quantum confinement effect permits the occurrence of distinctive physical and chemical interactions at the surface. Consequently, such morphological changes play a key role in controlling the electrical and optical properties of Nb_2O_5 which lead to unique or distinct observations that aren't common in bulk forms. Likewise, chemical and the physical properties of Nb_2O_5 can also be tailored using other ways

like; inclusion of foreign ions, post synthesis heat treatment and change of the crystal phase (Leviet *et al.,* 2010).

More recently, attention on Nb_2O_5 has gained more momentum due to applications in batteries, electronic devices like capacitors and photovoltaic (Graça *et al.,* 2015). Majority of these studies are still in their early stages and therefore much more research need to be done in order to discover the capabilities of Nb_2O_5. This will provide more insight to researchers who intend to conduct comprehensive studies on the application of this material in these areas (Michael *et al.,* 2014).

3.1.1 Crystal Structure of Niobium Pentoxide

Niobium pentoxide is a transparent material that is stable in air and insoluble in water with a rather complicated structure that exhibits wide-ranging polymorphism. It's clear from Table 3.1 that, low temperature synthesis method gives rise to amorphous Nb_2O_5. This crystallizes in to TT (pseudohexagonal) or T (orthombic) phases at approximately 500 ºC. At medium-temperature (800 ºC) the tetragonal also referred to as M phase is formed, and above 1000 ºC, the monoclinic or the H phase is formed (Raba *et al.,* 2016). In spite of the fact that temperature plays a big role in determining the crystal phase, other factors that may influence the formation of the final crystal are; process of preparation, nature of the precursor solution, presence of impurities and even interactions with other components. It's important to note that in some reports, crystal phases of Nb_2O_5 have been re-designated as α = H, β = M, and γ = T. Nevertheless, there are a lot of inconsistencies regarding the identification of Nb_2O_5 crystal phases. A few researchers proposed that the M phase is basically H phases that are dis-ordered while M-Nb_2O_5 has been reported as a tetragonal Nb_2O_5

phase (Michael *et al.*, 2014). Table 3.1 shows some of the properties of different Nb_2O_5 crystal phases.

Table 3.1: Properties of different Nb_2O_5 crystal phases (Michael *et al.*, 2014).

Crystal phase	Space group	Lattice constant a(Å)	b(Å)	c(Å)	Deposition Temperature (^oC)
Pseudohexagonal	P6/mmm	3.60	3.61	3.92	500
Orthormbic	Pbam	6.19	3.625	3.94	-
Tetragonal	*I*4/mmm	20.44	3.83	3.82	900
Monoclinic β=119.9^o±0.4^o	P12/m1,p 2,p2/m	21.14	3.82	19.45	>1000

3.2 Deposition Methods for Niobium Pentoxide Thin Films

The most common synthesis methods that are used to synthesize Nb_2O_5 are; the liquid phase deposition and vapor deposition methods.

3.2.1 Liquid Phase Deposition Methods

Liquid phase deposition is a method that uses aqueous solution under ambient conditions to produce thin films of oxides. Liquid phase techniques that are used to deposit niobium pentoxide thin films comprise processes like anodization, hydrothermal, sol-gel and electro-deposition.

3.2.2 Solvo-thermal Methods

Solvo-thermal method is a process that involves the use of a solvent under conditions of moderate to high temperature and pressure. Examples of solvents that may be used in this technique are isopropyl alcohol and acetone among others. If the solvent used is water, the process is referred to as hydrothermal synthesis. Solvo-

thermal and hydrothermal are simple methods that can be employed in the preparation of various geometries such as bulk powders, nanocrystals, single crystals and thin films. The methods include ionic form of metal that is constituted in a solution which is heated at high temperatures for a specified duration. In order to deposit Nb_2O_5, the solution of Nb^{5+} ions can be obtained through dissolution of niobium pentachloride among other niobium salts, or interaction of niobium metal in an acid or base. The solvent is heated at temperatures between 100^oC and 600^oC for a considerable duration that may range from a few to several hours or even several days. Usually, this procedure enhances the nucleation and formation of crystalline Nb_2O_5 to proceed. Some of the nanostructured configurations that can be obtained with hydrothermal and/ or solvo-thermal techniques include nanobelts, nanospheres and nanorods among others.

3.2.3 Anodization Technique

Anodization refers to the electrochemical process of oxidizing metals. It is a widely used nano- fabrication technique as it is capable of producing oxide morphologies that are highly porous. In an anodization process, normally two electrodes i.e. a working electrode (the anode) and a counter electrode which is usually a stable metal are employed. These electrodes are both immersed in a liquid electrolyte and a potential is applied between them. This enhances occurrence of electrochemical reaction on the surface of the anode resulting in the formation of an oxide film (Jacob, 2009).

Several factors such as anodization voltage employed, the electrolyte chemical composition, duration of anodization, and temperature of the electrolyte affect the

anodic oxide film formation and morphology. Nb_2O_5 film structure which is amorphous in nature is formed and therefore the necessity for post-annealing treatment in order that a highly crystalline and also stoichiometric Nb_2O_5 is formed.

3.2.4 Sol-gel Method

The other name for sol-gel process is chemical solution deposition method. It's a simple wet-chemical technique in which selected monomers are converted into a colloidal solution. The obtained solution is then used as a precursor in the formation of a gel. The gel is finally used for creating distinct particles or connected networks. In sol-gel process, the depositing of the final metal oxide films is usually done by techniques like dip coating spin coating and electro spinning. In spite of sol-gel being a simple method, it has some drawbacks like creation of weak bonds that result in lack of uniformity or homogeneity in films. Control of rate of reaction and also the porosity of the resulting film is also a challenge (Pierre, 1998).

3.2.5 Electro-deposition

Electro-deposition is a technique that is used to deposit nanostructured materials from a solution that contains ionic species. Materials fabricated using this method may be in powder form, thin films and composites. It comprises of three electrodes, i.e a reference electrode, the counter electrode and the working electrode. A potentiostat to which these electrodes are connected is used to control the deposition process; these electrodes are immersed in a solution that contains ionic species where after electric field is applied across the electrodes metal oxide film is formed at the working electrode (Physics and materials science research unit, 2017).

For Nb_2O_5 electro-deposition, niobium ions and H_2O_2 are normally contained in the aqueous electrolyte solution (Joo-Hee Jang *et al.,* 2011). The disadvantage with this method is that its time consuming and costly. Moreover it may cause environmental concerns with regard to the disposal of solutions used in the technique.

3.3 Vapor Phase Deposition

Vapor phase deposition is a method that involves fabrication of layers of materials from the condensation of their vaporized sources which is carried out under environments that are favorable. The main classes of vapour phase deposition include physical vapour deposition (PVD) and chemical vapour deposition (CVD).

3.3.1 Physical Vapor Deposition (PVD)

Physical vapour deposition (PVD) is essentially a vaporization coating technique used to produce thin films and coatings. The precursors are vaporised by physical means such as heat, bombardment ion, electron beam or laser irradiation. The vaporized atoms are transported to the substrate to be coated where it is deposited on the surface. The most widely reported PVD technique for depositing Nb_2O_5 is sputtering. In general, Nb_2O_5 films can be obtained using techniques such as direct current (DC) or radio frequency (RF) sputtering with metallic niobium (Nb) or Nb_2O_5 targets which utilize argon or other carrier gases within oxygen environment. Although sputtering technique is capable of producing high quality films, it consumes a lot of time because of low rates of deposition which can range in a μm per hour. Apart from sputtering, other PVD techniques that can be used to fabricate Nb_2O_5 films are pulsed magnetron sputtering, ion-beam assisted deposition, thermal evaporation and pulsed laser deposition (PLD).

However in general, Physical Vapour Deposition Process have disadvantages such as high capital cost, need of highly skilled operators because of the of some of the processes that operate at high temperatures and high vacuums, requires an elaborate cooling systems because of the large amounts of heat involved, and the rate of coating deposition is generally quite slow (AzoM, 2002).

3.3.2 Chemical Vapor Deposition (CVD)

Some of the CVD techniques that have been used to successfully synthesize Nb_2O_5 thin films are metal organic CVD (MOCVD), atmospheric pressure CVD (APCVD), plasma-enhanced CVD (PECVD), and vapour-liquid-solid (VLS) growth methods which may either be done under atmospheric conditions or vacuum conditions. $NbCl_5$ and pentaethoxy niobium [Nb $(OC_2H_5)_5$] are used as precursors for the deposition of Nb_2O_5 thin films. Normally, the precursor is conveyed to the chamber where reaction takes place by use of a carrier gas after which it undergoes decomposition on the heated substrate surface.

Spray pyrolysis is an aerosol assisted CVD technique. It is among the most widely used methods in the synthesis of thin or thick Nb_2O_5 films. This technique has the potential to produce thin films in large scale by employing simple apparatus. In cases where low temperatures are used during deposition, post annealing is necessary in order to obtain Nb_2O_5 thin films that are highly crystalline.

3.3.3 Spray Pyrolysis Deposition Technique

Spray pyrolysis is a process that is attractive for the deposition of inexpensive, thin-film photovoltaic solar cells (Krunks *et al.,* 2001). With this technique, it is possible

to deposit films that are layered and films with composition gradients throughout the thickness by altering the constituents of the spray solution and deposition parameters. Usually, a precursor aerosol is sprayed to the substrate during spray pyrolysis deposition process. A new chemical compound is formed when the constituents in the precursor react on the substrate surface. At the same time, some byproducts are formed which are vaporized to the atmosphere. The substrate temperature, the precursors' solution carrier gas, spraying rate, and the cooling rate after deposition influence the properties of the deposited film. Factors that influence the thickness of the film are temperature, the distance between the spray nozzle and the substrate, concentration of precursor solution, and the spray duration. The formation of the film depends on the evaporation of the reactant and the process of droplet landing. If the solvent is totally removed at the moment the droplet approaches the substrate, then ideal deposition is considered to have occurred (Patil, 1999).

3.4 Optical Reflectance

Reflection refers to a situation where a wave front changes direction when it hits the interface between two dissimilar media causing it to return to the medium from which it originated. Reflectance is the ratio of reflected power to incident power expressed as percentage. Reflection of light may be specular or diffuse. Specular reflection occurs on a blank mirroring surface that retains the geometry of the beams of light. Diffuse reflection occurs on a rougher surface, not retaining the imaging geometry, only the energy.

In measuring the reflectance of a thin film using spectrophotometer, incident light (I_i) of known wavelength is shone on to the surface of thin film and the intensity of reflected light (I_r) is measured. The intensities of the two are compared by the reference called reflectance (R) which is given by equation 3.1.

$$R = \frac{I_r}{I_i} x100 \qquad 3.1$$

3.5 Optical Transmittance

Optical transmittance refers to the amount of light transmitted by a surface normalized by the amount of flux incident to it. Any flux neither reflected nor transmitted is normally absorbed. When photons of specific wavelengths and light beam intensity strike a film, photons with energies larger than the band gap energies (E_g) of the film cause the excitation of electrons in the valence band to the higher states hence they are absorbed. Photons whose energies are less than the band gap do not cause excitation of the valence electrons and therefore they are transmitted.

Therefore transmittance (T) gives the relationship between the incident (I_o) photons to the transmitted photons (I_t) and it is given by equation 3.2.

$$T = \frac{I_o}{I_t} x100 \qquad 3.2$$

3.6 Semiconductor and Energy Bands

Semiconductor materials are categorized depending on their energy band structure. There are three distinct energy bands in a semiconductor material namely, valence band, conduction band, and the forbidden gap as illustrated in figure 3.1. In a semiconductor material, electrons contained in the conduction band possess energies

greater than conduction band lowest energy level (E_c). The number of holes in the valence band is equal to the number of electrons in conduction band. These holes have energies that are smaller than the valence band highest energy level (E_v).

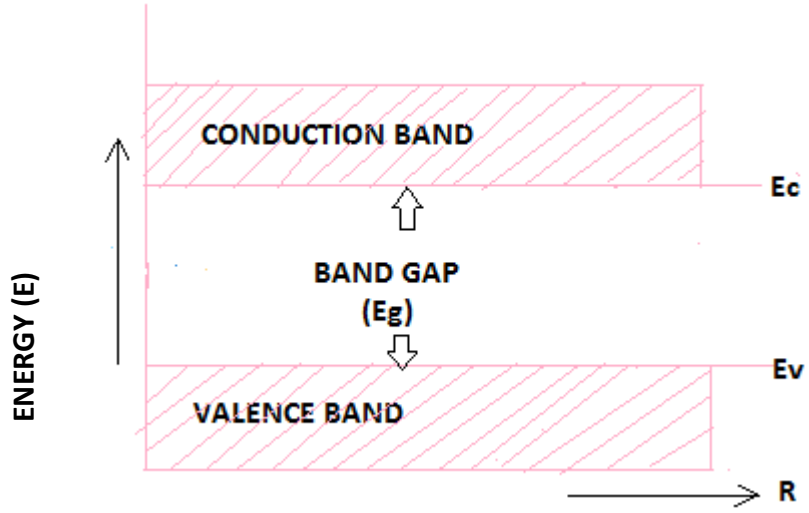

Figure 3.1: Energy diagram of a semiconductor

Band gap is the difference in energy between the conduction band edge E_c and the valence band edge E_v. No electron can stay in band gap because there is no allowed energy state in this region. The band gap of the semiconductor material can be calculated using equation 3.3

$$E_g = E_c - E_v \qquad 3.3$$

When electron- hole recombination occurs, energy is released which is the same as the original difference in the energies of the two charged particles. The energy thus realized is released as radiation. A photon is emitted if the radiation frequency is within the visible range and the process is referred to as radiative recombination. The emitted photon energy is given by equation 3.4

$$E = h\nu \qquad 3.4$$

where ν is the frequency of radiation and h is the Planck's constant (6.626×10^{-34} Js). If photon emission does not occur after recombination has taken place, then the process is referred to as non-radiative recombination. In a semiconductor material, electron-hole recombination is partly radiative and partly non-radiative. Radiation efficiency refers to the ratio of radiative combinations to the overall number of recombinations.

3.6.1 Direct and Indirect Band Gap

Based on the energy band diagram in the energy-momentum space, there are two types of semiconductor material namely indirect and direct band-gap semiconductor materials (Vajpeyi, 2010).

Figure 3.2 shows a schematic diagram of energy bands of direct and indirect semiconductors. In a direct band-gap semiconductor, the highest energy level of valence band takes place at the same value of momentum with the lowest energy level of the conduction band while in indirect band gap semiconductor, these two levels of energy are not aligned as far as momentum is concerned. In a direct band gap semiconductor, a direct recombination occurs and in the process energy that is equal to the difference in energy between the particles recombining is released.

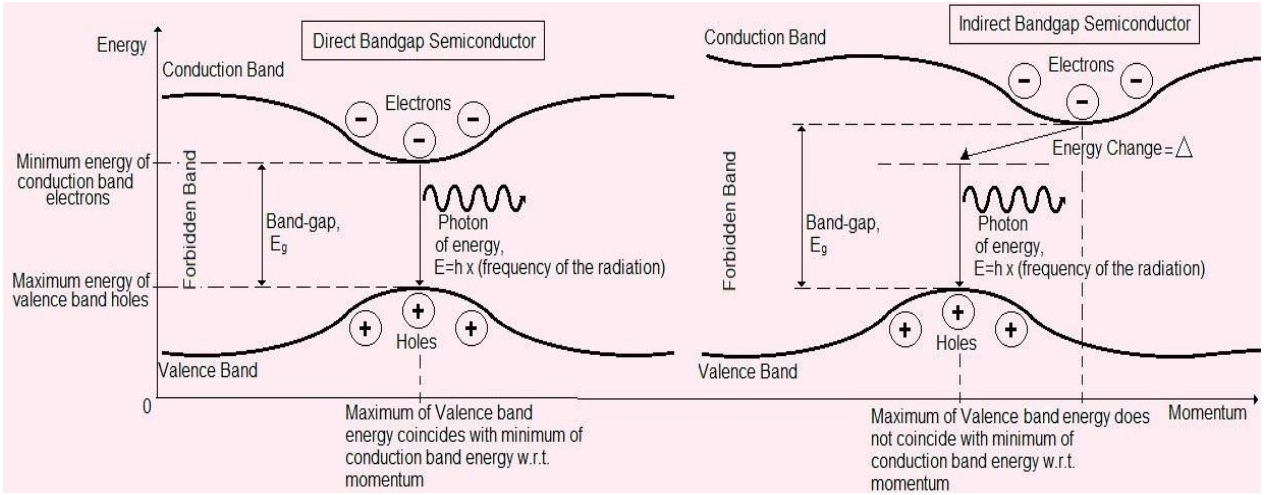

Figure 3.2: Energy band diagram of a semiconductor (Shevgaonkar, 2012).

When it comes to indirect band gap semiconductor, there is a relative difference in momentum and as a result, the momentum is first conserved through the release of energy. Recombination can only take place when the two momenta come to an alignment. Hence, the chances of radiative recombination occurring in an indirect band gap semiconductor are much less as compared to direct band gap semiconductors. Thus, efficiency factor of a direct band gap semiconductor is great as compared to that of an indirect band gap semiconductor. That is the reason why in making optical sources, direct band gap semiconductors are always preferred as opposed to indirect band gap semiconducters (Vajpeyi, 2010).

3.7 The Absorption Coefficient

The absorption coefficient (α) is a property of a material that defines the amount of light of a particular wavelength absorbed by it. Light is poorly absorbed in materials with a low absorption coefficient, and very thin materials appear transparent to the wavelength. The type of material and the wavelength of light that is being absorbed greatly influence absorption coefficient. Semiconductor materials have a sharp edge

in their absorption coefficient, because light with energy below the band gap does not have enough energy for electron excitation from valence band in to the conduction band. As a result light absorption does not take place. The probability of photon absorption depends on the possibility of having a photon and electrons interact in such manner so as move from one energy band to another.

Absorption is relatively low for photons which posses energy very close to that of the band gap, as its only those electrons directly at the valence band edge can interact with the photon for absorption to occur. Semiconductors with direct energy gap are generally characterized by a high absorption coefficient in the relevant energy range for photovoltaic's. Most of the sunlight is absorbed within a small range beneath the surface, hence possibility to fabricate thin film solar cells. Indirect semiconductors need more material to absorb most of the sunlight and therefore thicker layers are needed. The relationship between absorption coefficient (α) and extinction coefficient (k) is given by

$$\alpha = \frac{4\pi k}{\lambda} \qquad 3.4$$

where λ is the wavelength.

3.8 XRD Structural Analysis

The use of X-rays for the structural analysis is based on the fact that waves undergo diffraction when they interact with systems (diffraction centers) which are spaced at distances of the same order of magnitude as the wavelength of the particular radiation considered. X-ray diffraction in crystalline solids takes place because the atomic spacing's are in the 10^{-10} m range, as are the wavelengths of X-rays.

When beams of X ray are incident to plane of crystal of a solid, they are scattered from the crystal lattice. The peaks of the scattered intensity are produced which correspond to the angle of incident which is equal to the angle of scattering. The path length difference is equal to an integer number of wavelengths. Constructive interference for parallel planes of atoms that has a space of d_{hkl} between the planes only occurs when Bragg's law is satisfied as shown in equation 3.5 (Donald, 2009).

$$n\lambda = 2d\sin\theta \qquad 3.5$$

Braggs law relates the angle θ (at which there is maximum diffracted intensity) to the wavelength λ of the X rays and the inter distance d between the planes of molecules/or atoms in the lattice.

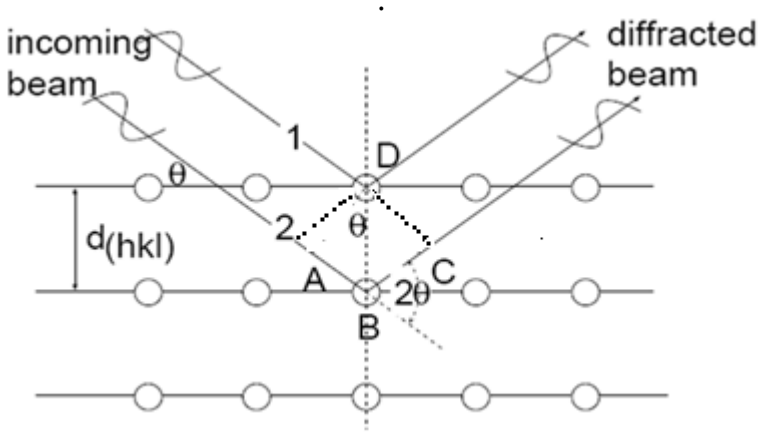

Figure 3.3: Bragg reflection from a particular family of lattice planes

The scattering of the x-rays from atoms produces a diffraction pattern which contains the information about the atomic arrangement of the crystal.

In our diffractometers, the X-ray wavelength (λ) is fixed. As a result, a family of planes produces a peak of diffraction only at a specific angle θ. In addition to this; the plane normal should be parallel to the diffraction vector (Donald, 2009).

CHAPTER FOUR

MATERIALS AND EXPERIMENTAL PROCEDURES

4.1 Introduction

In this section the steps for producing Nb_2O_5 thin films is described. The film preparation included depositing Nb_2O_5 layer on glass substrate by spray pyrolysis technique. Kovendhan *et al*. (2011) method was employed but with varied substrate temperature and spray duration.

4.2 Cleaning of the Substrate

The substrates material used in this study were ordinary microscope glass slides. In order to remove dirt from the glass substrates, they were cleaned ultrasonically. This technique involves the use of high frequency sound waves which are applied in a liquid. The ultrasonically activated liquid removes any foreign contaminants from the surfaces of the films submerged in it.

In this work, the glass substrates were cleaned in a detergent solution under sonication for 15 minutes, after which they were rinsed with distilled water, followed by sonication again in distilled water and rinsed again with distilled water then let to dry in open air. Figure 4.1 shows a picture of the sonicater that was used.

Figure 4.1: Sonicator machine

4.3 Preparation of Precursor Solution

A solution of niobium pentachloride was prepared by dissolving niobium pentachloride in distilled water, to which hydrogen peroxide and acetic acid were added as tabulated in Table 4.1.

4.4 Preparation of the Films

Prior to the deposition, the glass substrates were heated after which spraying of $NbCl_5$ solution was done on the glass substrates using the automated spray pyrolysis machine shown in figure 4.2. It had a standard substrate to nozzle distance of 13 cm. The main parts of spray pyrolysis equipment are represented in figure 4.3. The films were sprayed at temperatures of 270^{o}C, 370 ^{o}C, and 470 ^{o}C at duration of 1min, 2

min, and 3 minutes respectively. Boiling point of $NbCl_5$ and the structural phase formation of Nb_2O_5 which would influence light absorption in a DSSC photo anode were considered in selecting the substrate temperatures.

Table 4.1: Preparation of precursor solution

	Parameter	**Optimal value**
1.	Solvent	0.5g(0.00185moles) of $NbCl_5$ in 90ml of H_2O+10 ml H_2O_2+1ml of 17.47M glacial
2.	Nozzle to Substrate distance	13 cm
3.	Spray duration	1 min, 2 min& 3 min
4.	Temperature	270^oC, 370^oC & 470^oC
5	Pressure	6 bar

The Air blast atomizer was used. Before the spraying could be done, the air pressure from the spraying nozzle was varied between four bars to eight bars in order to obtain the optimal value to be used. At a value of four and five bar, the pressure was not sufficient to atomize fully the precursor solution and therefore such could cause the precursor liquid to just spill on the substrate. At values of seven bars and eight bars, the pressure was too much to a point of splashing the precursor solution away from the substrate surface. Therefore a standard pressure of 6 bars was used for making all the films as films that adhered well to the substrate surface were being obtained.

Nb_2O_5 was obtained by hydrolysis of $NbCl_5$. Hydrolysis is the braking of a compound by use of water. This was done in presence of H_2O_2 and acetic acid as the catalysts.

The water hydrolyze $NbCl_5$ as shown in equation 4.1 leading to the formation of Nb_2O_5

$$2NbCl_5 + 5\ H_2O \rightarrow Nb_2O_5 + 10HCl. \qquad 4.1$$

HCL is highly volatile and therefore it vaporizes in air.

Figure 4.2: Automated spray pyrolysis equipment

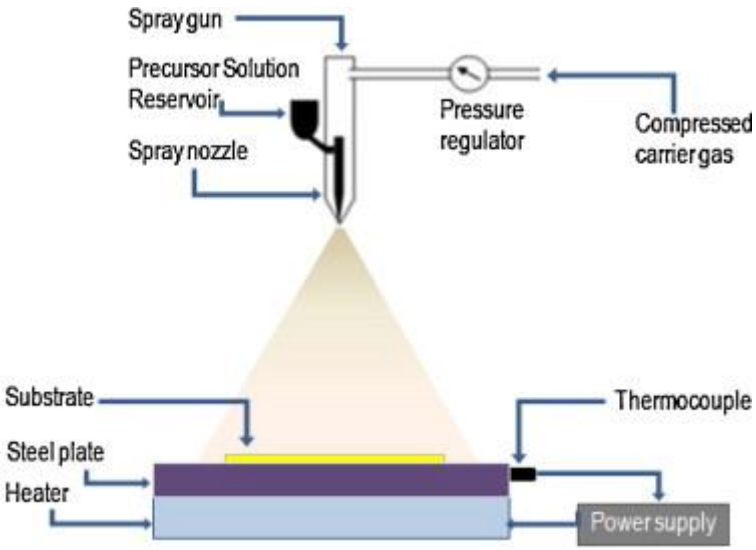

Figure 4.3: Scheme of the spray pyrolysis setup

4.5 Characterization

The sprayed solution underwent thermal decomposition which resulted in formation of niobium pentoxide thin films which adhered very well on the substrate surface.

4.5.1 Optical Characterization

Optical characteristics of the Nb_2O_5 thin films were characterized using Shimadzu model type DUV 3700 spectrophotometer shown in figure 4.4 for un-polarized light. Data for transmittance, and reflectance was collected at wavelength range 200 nm – 2500 nm. The graphs for transmittance and reflectance were then plotted using Microcal OriginLab^{TM} software. The thicknesses of the films were estimated using the KLA Tencor Alpha –step IQ surface profiler. PUMA software was used in analyzing the collected data in order to calculate the absorption coefficient and band gap energy of Nb_2O_5. Absorption is expressed by absorption coefficient (α) which is

relative rate of decrease in light intensity along the propagation path. Absorption coefficient is expressed by Beer's law given by equation 4.2

$$I_t = I_o e^{-\alpha d} \tag{4.2}$$

Therefore

$$\alpha = \frac{1}{l} \ln\left(\frac{I_o}{I_t}\right) \tag{4.3}$$

where I_t is the transmitted light intensity, I_o is the incident light intensity, and l is the thickness of the thin film.

Figure 4.4: DUV 3700 solid spectrophotometer

4.5.2 Estimation of energy band gap

Energy band gap of the prepared Nb_2O_5 thin films was obtained from spectral plot of absorption coefficient versus photon energy. Absorption coefficient is related to photon energy according to equation 4.4

$$\alpha = \frac{\alpha_0 (h\upsilon - E_g)^n}{h\upsilon} \qquad 4.4$$

where E_g is the separation between bottom of the conduction band and top of the valence band and hν *is* the photon energy. α_o is the constant for direct transition and n is a constant which depends on the probability of transition (Kun-Neng *et al.*, 2016). The value of n is different and it has values of 1/2 for direct allowed, 3/2 for direct forbidden, 2 for indirect allowed and 3 for indirect forbidden transition. The incident photon energy (E=hν) is calculated as a function of wavelength (λ) from equation 4.5 (Daniel, 1999).

$$h\upsilon = \frac{1240}{\lambda} \text{ (eV.nm)} \qquad 4.5$$

Nb_2O_5 is a direct energy band gap material (Kun-Neng *et al.*, 2016). Hence, substituting the value of n=1/2 in equation 4.4 we have

$$\alpha = \frac{\alpha_o (h\nu - Eg)^{1/2}}{h\nu} \qquad 4.6$$

Therefore, if a plot of $(\alpha h\nu)^2$ against $(h\nu)$ is linear, then the transition is direct allowed (direct band gap). Estimation of the band gap is done by extrapolating the straight-line portion to $(\alpha h\nu)^2 = 0$ as shown in figure 4.5.

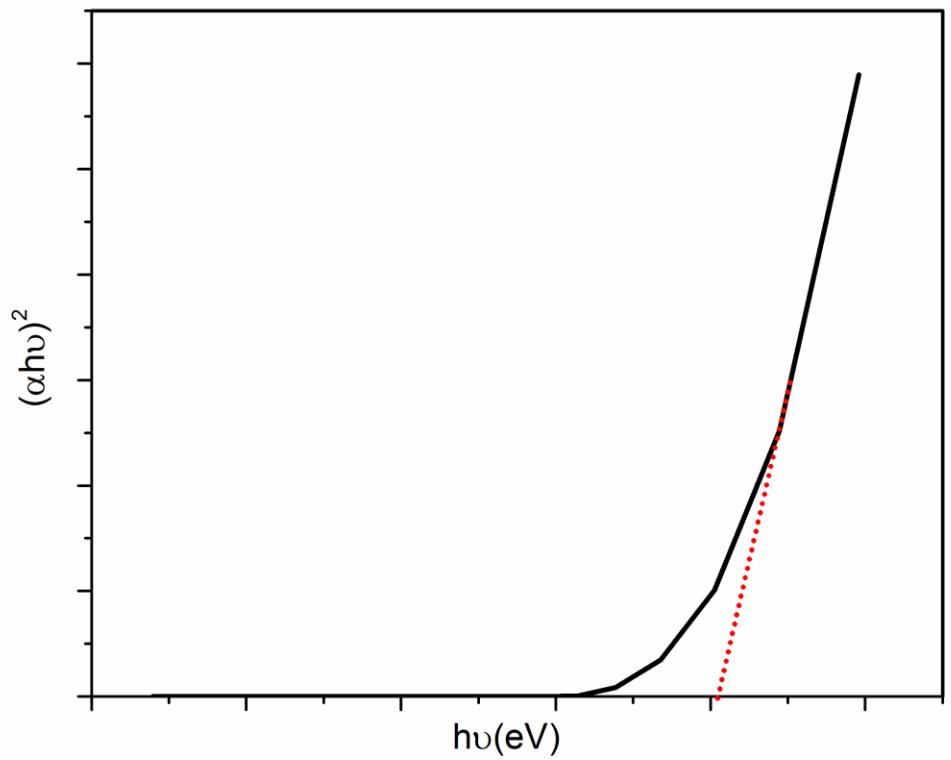

Figure 4.5: A plot of $(\alpha hv)^2$ versus (hv) for Nb_2O_5 thin film.

4.6 Sheet Resistivity

It is the measure of resistance of two dimensional film of uniform thickness. The measurement is used in describing surface resistance of semiconductor materials. Unit used is ohm/square. Thickness must be very small as compared to the lateral dimension of the film and the contacts must be very small and made from the same material. Sheet resistance of the prepared niobium pentoxide thin films were measured using the four points probe method whereby keithy 2400 source meter was employed for this purpose.

Figure 4.6 shows a schematic sketch of the four point probe configuration. A high impedance current source was used to supply current (I) through the outer probes while a voltmeter was used to measure the voltage (V) across the inner probes. The sheet resistance and hence the resistivity were determined from the measured values of current and voltage. For thin layers thickness is much less compared with the lateral dimension of the film i.e. t<<s and current rings are considered instead of spheres and therefore the expression for the area is A=2πxt.

The differential resistance is

$$\Delta R = \rho \frac{dx}{A} \qquad 4.7$$

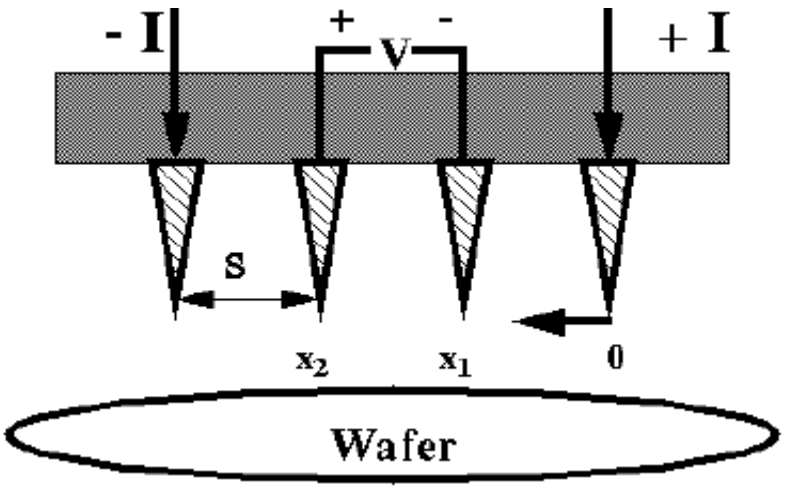

Figure 4.6: Schematic diagram of four point probe configuration (Friedberg, 2002).

Carrying out integration between the inner probe tips

$$R = \int_{x1}^{x2} \rho \frac{dx}{2\pi x t} = \int_{s}^{2s} \rho \frac{dx}{2\pi t x} = \frac{\rho \ln 2}{2\pi t} \qquad 4.8$$

Because of the superposition of current at the outer tips

$$R = \frac{V}{2I} \tag{4.9}$$

Substituting equation 4.9 into equation 4.8 and making ρ the subject of the formula, we have

$$\rho = \frac{\pi t}{\ln 2}\left(\frac{V}{I}\right) \tag{4.10}$$

where ρ is the resistivity, t is the film thickness; V and I are the measured voltage and current respectively (Friedberg, 2002).

Equation 4.10 can also be written as

$$\rho = 4.5324\frac{V}{I}t \tag{4.11}$$

Sheet resistivity of the prepared Nb_2O_5 thin films was calculated using equation 4.11.

4.7 XRD Characterization

The Bruker D2 phaser XRD was used to measure the diffraction pattern of the sample. It had Cu radiation (30 kV, 10 mA) X-ray tube, and was mounted with Ni filter and a LYNXEYE detector opening 5° 2Theta. It had a Continuous scan from 4 to 45° 2Theta and 0.02° step width. Total counting time per step was 2.5 sec and overall scan time was about 45 min. The instrument also had 2.5° Soller collimators, 0.6 mm divergence slit, and an anti-scatter screen. The obtained XRD pattern was analyzed using COD.

The average crystalline size D was estimated using the scherrer equation as follows;

$$D = \frac{K\lambda}{\beta \cos\theta} \qquad 4.12$$

Where k is a dimensionless shape factor that has a typical value of about 0.9, λ is the wavelength of the x-ray radiation in nm, β is the line broadening at half the maximum intensity (FWHM) in radians and θ is the Braggs diffraction angle in degrees.

FWHM was determined by identifying the two points on each of the highest peaks of the x-ray diffraction spectra where the curve was at half its maximum value as illustrated in figure 4.7

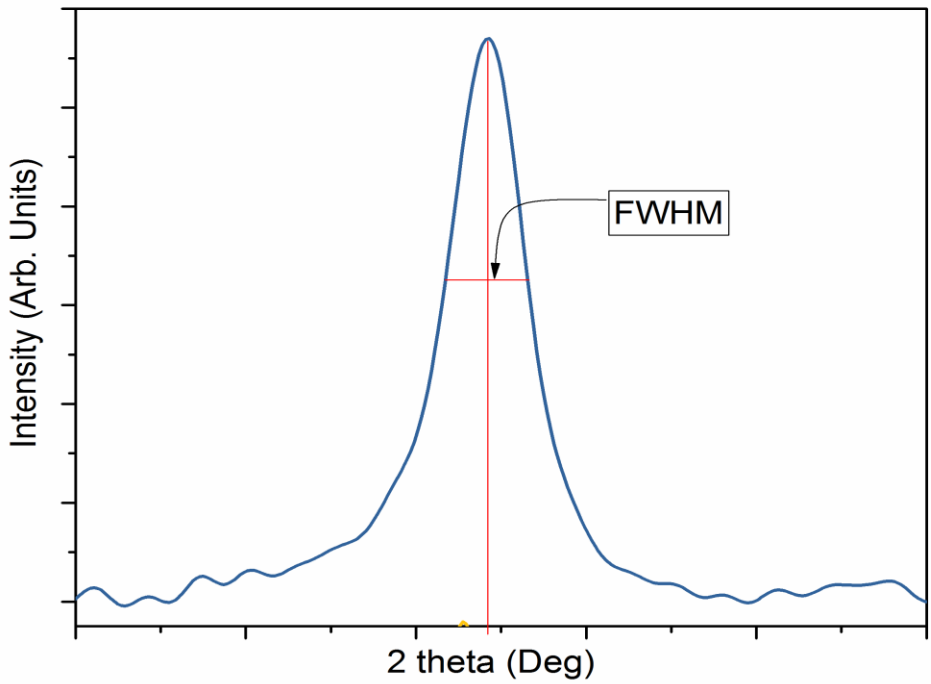

Figure 4.7: Determination of FWHM of Nb_2O_5 thin film.

CHAPTER FIVE

RESULTS AND DISCUSSION

5.1 Optical Spectra of Thin Films

Experimental data for transmittance and reflectance was obtained from shimadzu model DUV 3700 spectrophotometer using the UV probe software. It was converted in to Microsoft excel and then used to plot graphs of transmittance and reflectance for niobium pentoxide thin films sprayed at different temperatures and durations.

5.2 Optical characteristics

5.2.1 Effect of spray duration on transmittance and reflectance of niobium pentoxide thin films

Figures 5.1(a) and 5.1(b) show the curves of transmittance and reflectance of niobium pentoxide thin films sprayed at 1min, 2min and 3min respectively at constant temperature of 270^{o}C. The average transmittance lies between 65% and 75% within the visible region and average reflectance is below 20%. It is observed that with increase in spray duration, the percentage transmittance decreases with a corresponding increase in percentage reflectance. This could be attributed to increased film thickness due to the intense formation of niobium pentoxide on the glass substrate as more material means larger thickness which in turn attenuates light rays.

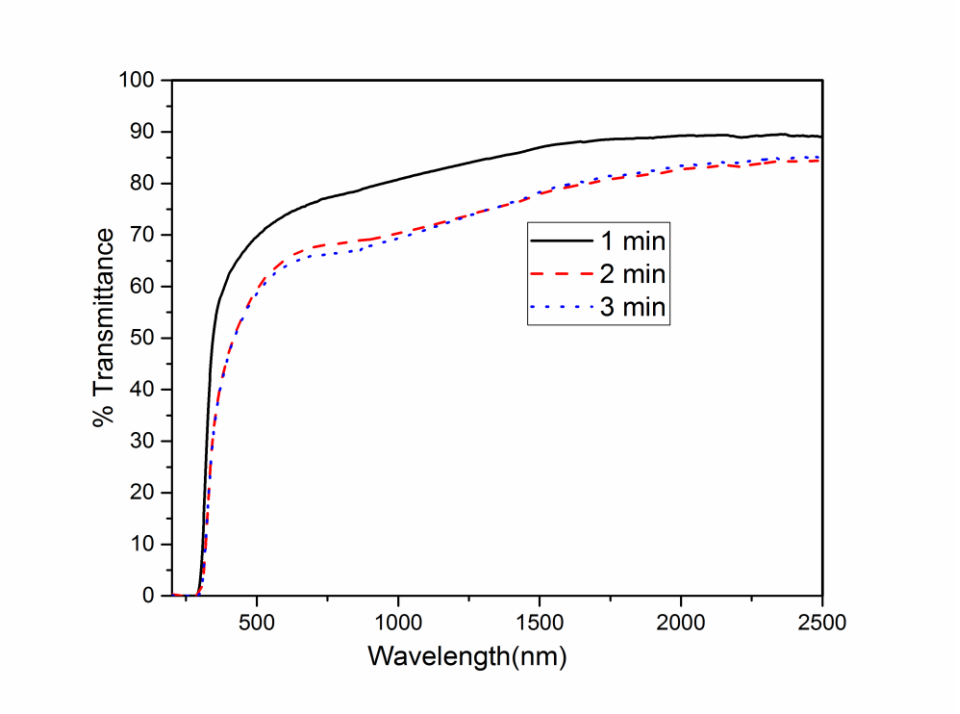

Figure 5.1: (a) Transmittance of Nb_2O_5 thin films sprayed at a temperature of 270^{o}C

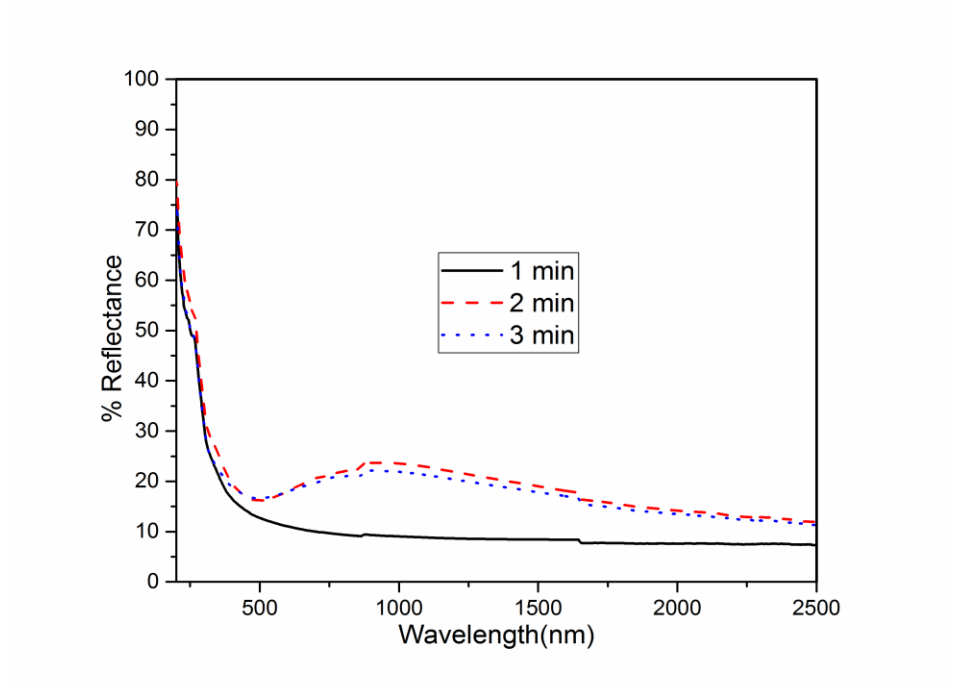

Figure 5.1: (b) Reflectance of Nb_2O_5 thin films sprayed at a temperature of 270^{o}C

Figure 5.2 a and 5.2 b shows the transmittance and reflectance spectra of niobium pentoxide thin films sprayed at a temperature of 370^{o}C at durations of 1 minute, 2 minutes and 3 minutes. It is observed that average transmittance lies within 60% and 65% and the reflectance is between 20% and 25 % within the visible region. The curves have a similar trend as for those films sprayed at 270^{o}C. However in both cases there is less effect in transmittance and reflectance as duration is increased from 2 minutes to 3 minutes. This could be due to the decrease in the rate of deposition at 3 minutes. This is expected because as the spray duration is increased, the kinetic energy of air molecules within the vicinity of the substrate increases which in turn bombards the precursor solution molecules on their way to the substrate surface.

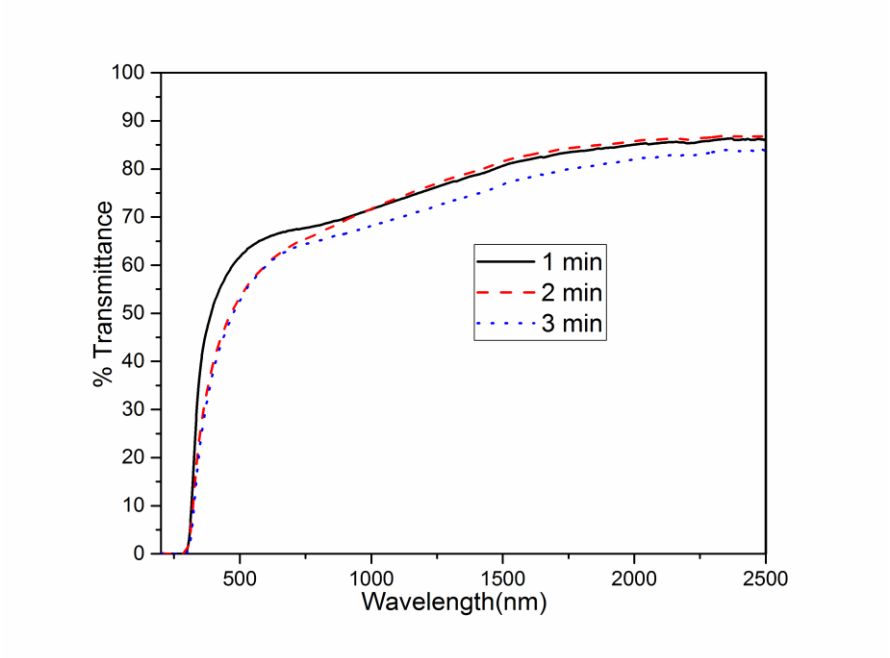

Figure 5.2: (a) Transmittance of Nb_2O_5 thin films sprayed at a temperature of 370^{o}C

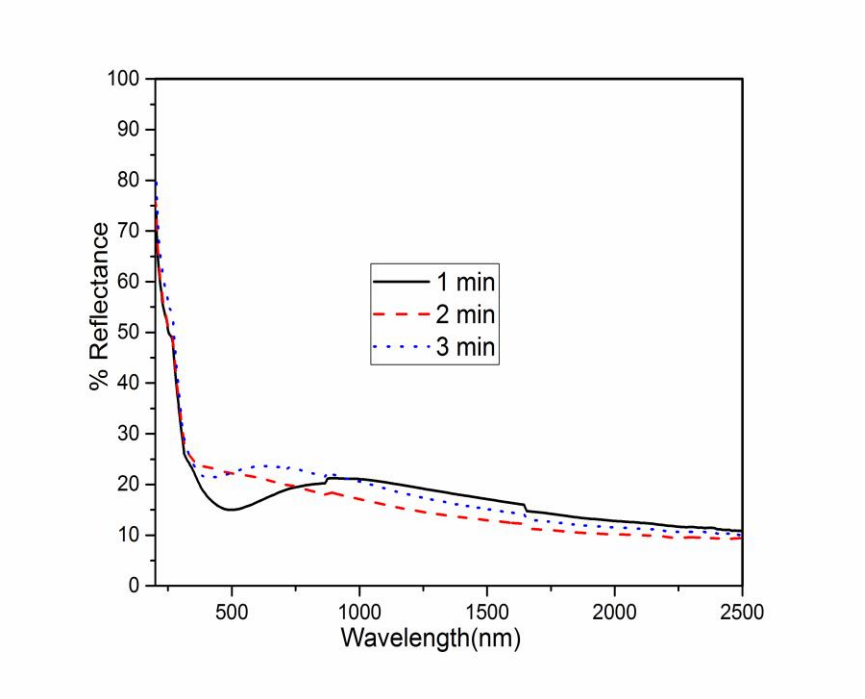

Figure 5.2: (b) Reflectance of Nb_2O_5 thin films sprayed at a temperature of 370^oC

Figure 5.3 a and 5.3 b are transmittance and reflectance spectra of niobium pentoxide thin films sprayed at a temperature of 470^oC at durations of 1min, 2min and 3min. Transmittance was again observed to decrease with increase in spray duration while the reflectance reduced. At 1 minute, average transmittance is about 90% while average reflectance is about 10%. This indicates that the light that was not transmitted was reflected and therefore absorption could not take place. At 2 min and 3 min, transmittance is between 70% and 80% and average reflectance was 10%. Therefore light absorption occurred at these durations.

.

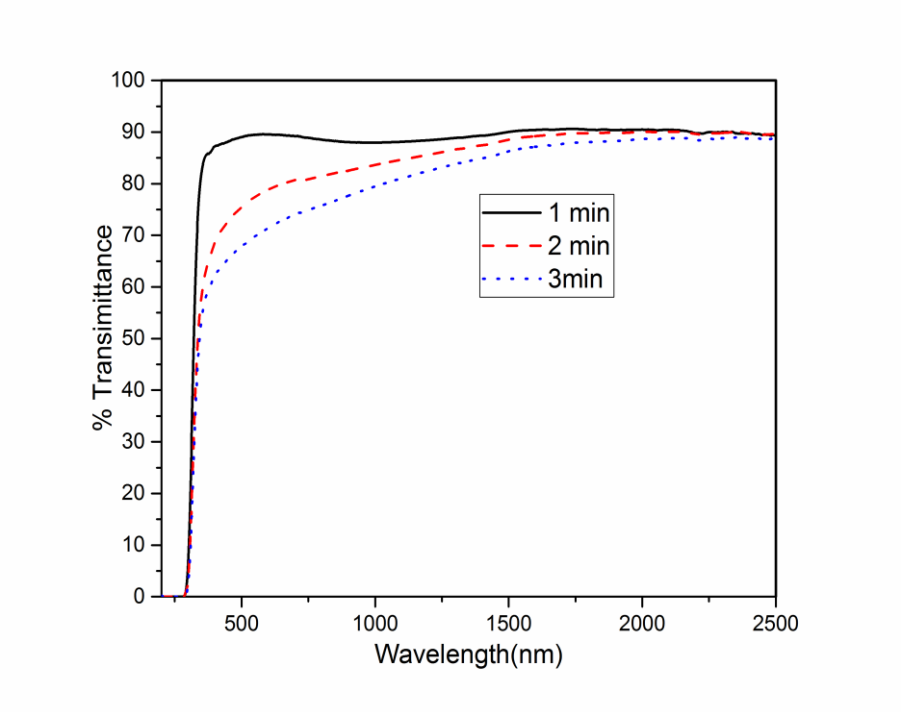

Figure 5.3: (a) Transmittance of Nb_2O_5 thin films sprayed at a temperature of 470^{o}C

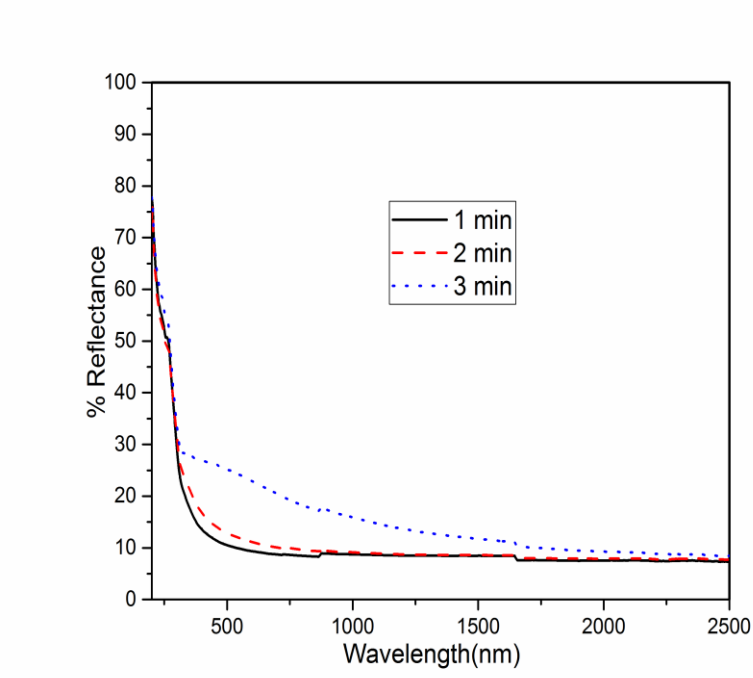

Figure 5.3: (b) Reflectance of Nb_2O_5 thin films sprayed at a temperature of 470^{o}C

5.2.2 Effect of temperature on transmittance and reflectance

Curves of niobium pentoxide thin films sprayed at 270^{o}C, 370^{o}C and 470^{o}C at constant duration of 2 min were also plotted in order to establish the effect of temperature on transmittance and reflectance. Results from figure 5.4 (a) and 5.4 (b) showed that films sprayed at temperature of 470^{o}C had the highest transmittance and the lowest reflectance followed by those films sprayed at 270^{o}C and 370^{o}C respectively. This could be attributed to reduction in thickness of the film at high temperatures as a result of increased rate of evaporation of precursor solution before it reached substrate surface (Patil *et.al.*, 2005).

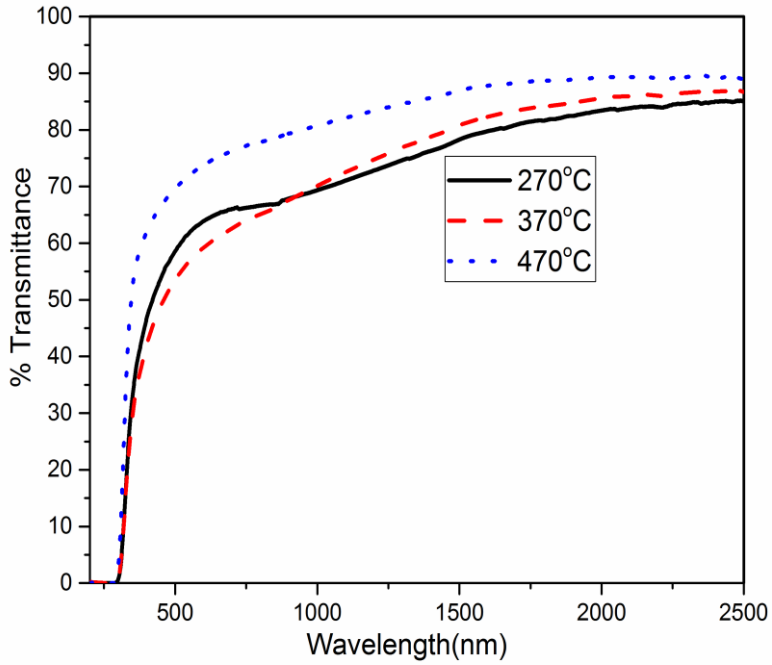

Figure 5.4: (a) Transmittance of Nb_2O_5 thin films sprayed at duration of two minutes

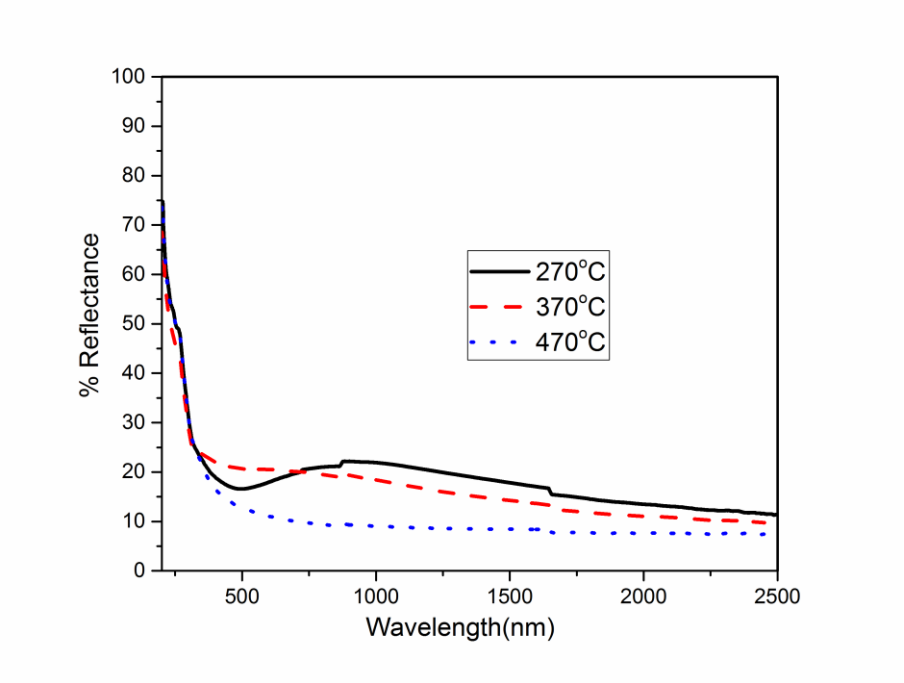

Figure 5.4: (b) Reflectance of Nb_2O_5 thin films sprayed at duration two minutes

High transmittance at 270°C indicates that the rate of deposition was low as compared to rate of deposition at 370°C, thus more material was deposited at 370°C. At 270°C, the temperature was not sufficient to enhance rapid decomposition of the precursor solution at the substrate surface (Sandeep and Dhananjaya, 2015). The absorption edge of the films is observed at around 300nm.

5.2.3 Effect of spray duration and temperature on the thickness of Nb_2O_5 thin films

Table 5.1 shows the thickness of films sprayed at duration of 1 min, 2 min and 3 min respectively. It is observed from the table that thickness of film increases with increase in spray duration this is due to increase in quantity of the precursor solution sprayed. However with temperature, the thickness is seen to first increase at 370°C then decreases at 470°C as shown in Table 5.2. This is due to the fact that as

temperature is increased, the rate of thermal decomposition of the precursor solution increases and more material is deposited. Further increase in temperature reduces thickness and this can be attributed to evaporation of the initial constituents of the precursor solution before it reached the substrate surface.

Table 5.1: Variation of thickness of Nb_2O_5 thin films with duration

Temperature(^oC)	Duration(min)	Thickness (nm)
270	1 min	281
	2 min	404
	3 min	444
370	1 min	284
	2 min	470
	3 min	517
470	1 min	162
	2 min	277
	3 min	414

Table 5.2: Variation of thickness of Nb_2O_5 thin films with temperature

Temperature(^oC)	Duration(min)	Thickness (nm)
270	2 min	404
370	2 min	470
470	2 min	277

5.3 Absorption coefficient.

Figure 5.5 shows plot of $(\alpha hv)^2$ versus photon energy for a niobium pentoxide thin film. It is observed that absorption coefficient is low at low photon energies and high

high photon energies. This indicates that light at short wavelengths was not well absorbed.

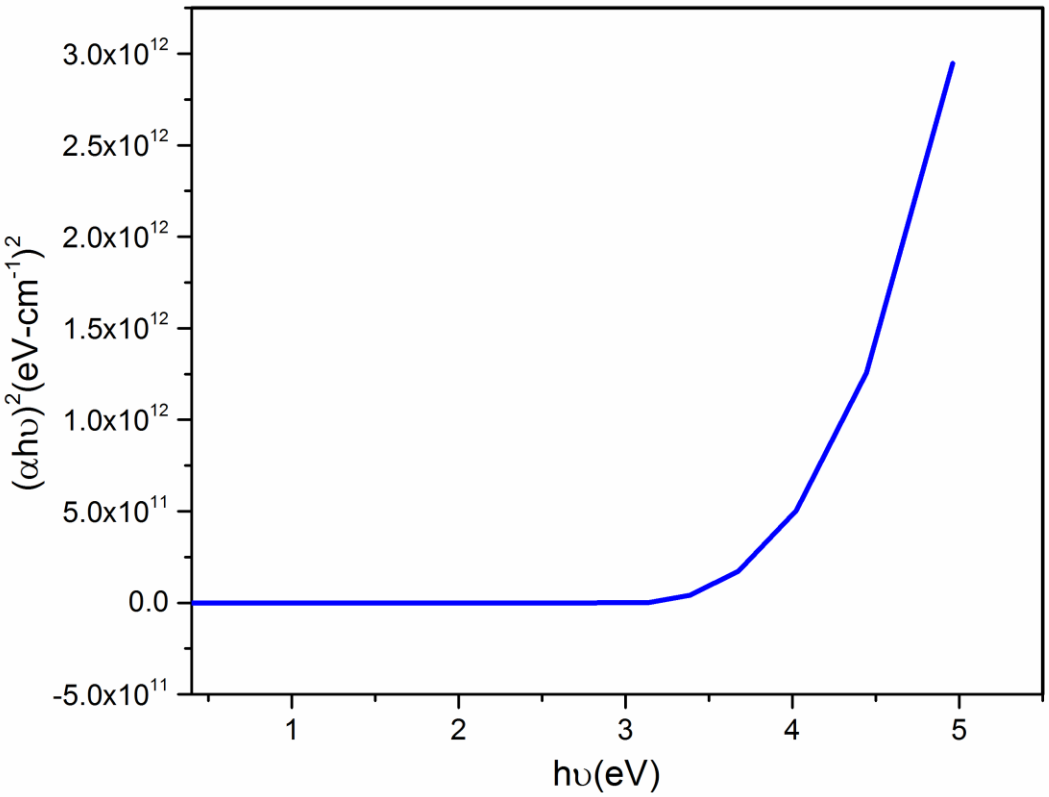

Figure 5.5: $(\alpha h\nu)^2$ versus photon energy curve for Nb_2O_5 thin film deposited at 470^{o}C at a spray duration of two minutes.

5.3.1 Energy band gap

The energy band gap values for the Nb_2O_5 thin film estimated as shown in figure 4.5 in section 4.5.2 lies between 3.92 and 4.12eV. Differences in band gap values were insignificant. Table 5.3 shows values of band gap obtained for niobium pentoxide thin film sprayed at different substrate temperatures and different durations. The band gap values obtained in this work are slightly higher than that reported by Kovendhan *et. al* (2011) but lie within the values reported by Brayner *et. al* (2003)

and Amita and Singh (2013). The increase in band gap can be attributed to the smaller crystalline size (Kovendhan *et.al.*, 2011).

Table 5.3: Band gap values for Nb_2O_5 thin film sprayed at different substrate temperatures and different durations

Substrate temperature(^{0}C)	Spray duration (minutes)	Band gap (eV)
270^{o}C	1min	4.11
	2 min	4.12
	3 min	4.03
370^{o}C	1min	4.02
	2 min	3.92
	3 min	3.95
470^{o}C	1min	4.01
	2 min	4.03
	3 min	3.98

5.4 Electrical properties

Table 5.4 shows the determined values of Nb_2O_5 thin films sheet resistivity with changing substrate temperature at a constant duration of two minutes. It is observed that with increase in temperature, the sheet resistivity decreases. This could be attributed to the increase in carrier concentration as temperature is increased (Jung-Ruey *et. al.,* 2105).

Table 5.4: Variation of sheet resistance of Nb_2O_5 thin films with temperature at a spray duration of two minutes

Film Deposited at	Current Range(mA)	Voltage Reading(mA)	Sheet Resistance (ohm sq)	Sheet resistivity (Ω cm)
470^{o}C	1	7.79166	35.31495	$9.8X10^{-4}$
370^{o}C	1	9.98533	45.25752	$2.1X10^{-3}$
270^{o}C	1	12.43833	56.37550	$2.3X10^{-3}$

Values for sheet resistivity were also determined for niobium pentoxide thin films sprayed at constant temperature but with varying spray duration. There is clear indication in table 5.5 that increase in spray duration led to increase in sheet resistivity. This is due to increase in film thickness and it agrees with equation 4.11 in section 4.6. From the obtained values of resistivity, it's clear that the deposited niobium pentoxide thin films exhibited semiconductor property.

Table 5.5: Variation of sheet resistance of Nb_2O_5 thin films with duration at substrate temperature of 470^oC

Film Deposited at	Current Range(mA)	Voltage Reading(mA)	Sheet Resistance (ohm sq)	Sheet resistivity (Ω cm)
1 min	1	9.89725	44.4800	$7.2X10^{-4}$
2 min	1	7.79166	35.31495	$9.8X10^{-4}$
3 min	1	9.34450	42.35641	$1.8X10^{-3}$

5.5 Structural Characteristics

The phase formation of niobium pentoxide was confirmed by use of XRD. The structure formed was found to be tetragonal with well defined reflections at (220) and (211). The corresponding lattice parameters are a= 20.4400 and Å c= 3.8320 Å respectively.

Figure 5.6 shows XRD graphs for films deposited 270^oC, 370^oC, and 470^oC. It is observed that there is increase in crystallinity with increase in temperature. Increase in the peak intensity shows that the films become more polycrystalline (Patil *et al.*, 2005). It is also seen in figure 5.7 that with increase in spray duration, peak intensity increases. This could be attributed to increase in crystallinity as a result of uniform distribution of temperature at 2 minutes and 3 minutes.

Moreover, more material is deposited which results to additional layers in the film that makes the peaks deposited at these durations to be intense (Isrihetty *et. al.*, 2010). The high crystallinity obtained in Nb_2O_5 films sprayed at 470^oC indicates

their suitability as an anode in DSSC application. This is because the crystalline surface would enhance light scattering and absorption within the semiconductor material.

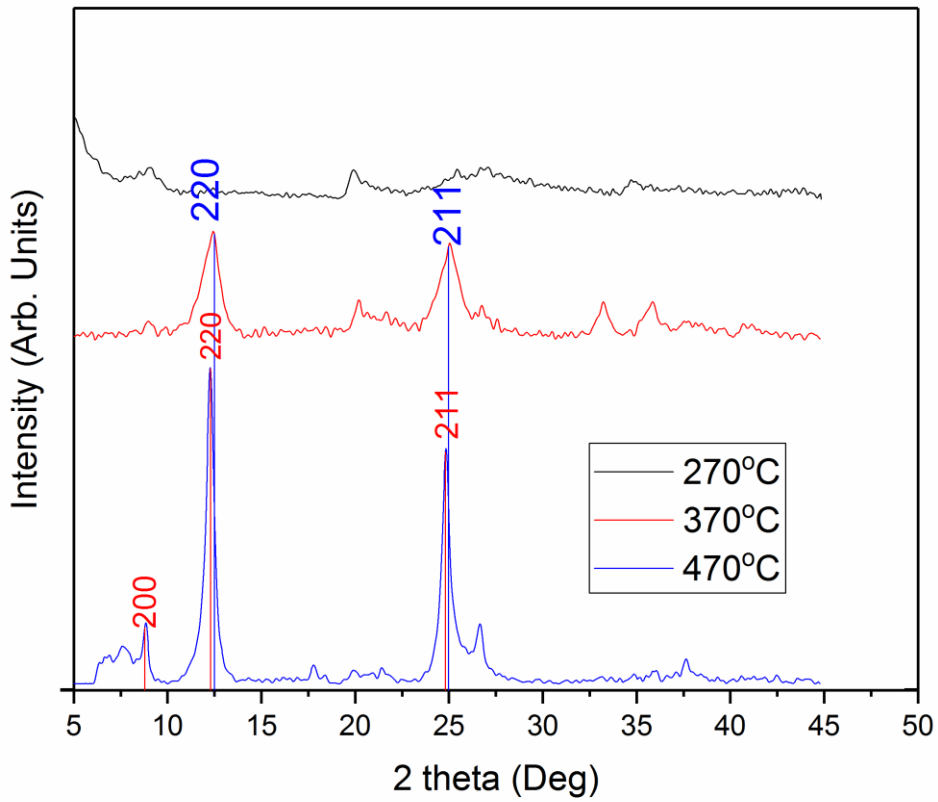

Figure 5.6: X-ray Diffraction pattern of Nb_2O_5 thin films deposited at 270^{o}C, 370^{o}C and 470^{o}C at a spray duration of two minutes

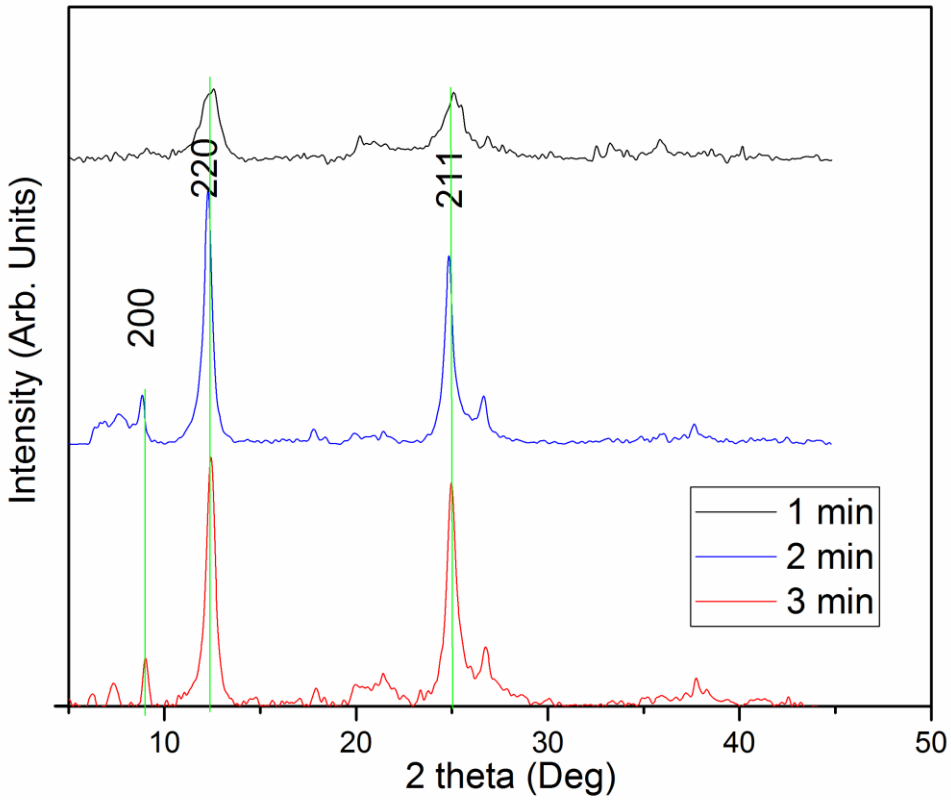

Figure 5.7: X-ray Diffraction patterns of Nb_2O_5 thin films deposited at 1 min, 2 min and 3 min at a substrate temperature of 470^{o}C.

Crystalline size

Table 5.6 gives crystal size of the samples derived from the full width at half maximum (FWHM) of the preferred orientation of the (220) and (211) phases. These are points which had high peak intensity and constructive interference was believed to have been at its maximum. For instant Figure 5.8 represents the FWHM for the highest peak that occurred at 12.39^{o}. The average crystalline size is found to be 21.25 nm. This value is slightly less than that obtained by Kovendhan *et. al* 2011.

Table 5.6 Crystal size derived from FWHM at the orientation of 220 and 211 planes

2θ	θ	Cosθ	FWHM(θ)	FWHM(rad)=β	βcosθ	Crystallite size(nm)
12.39	6.195	0.9941	0.3927	0.006853	0.006800	21.25
25.06	12.530	0.9761	0.4360	0.007610	0.007428	19.49
12. 41	6.210	0.9941	0.4651	0.008117	0.0080609	1 7.96
24.87	12.435	0.9765	0.4479	0.007717	0.007634	18.98

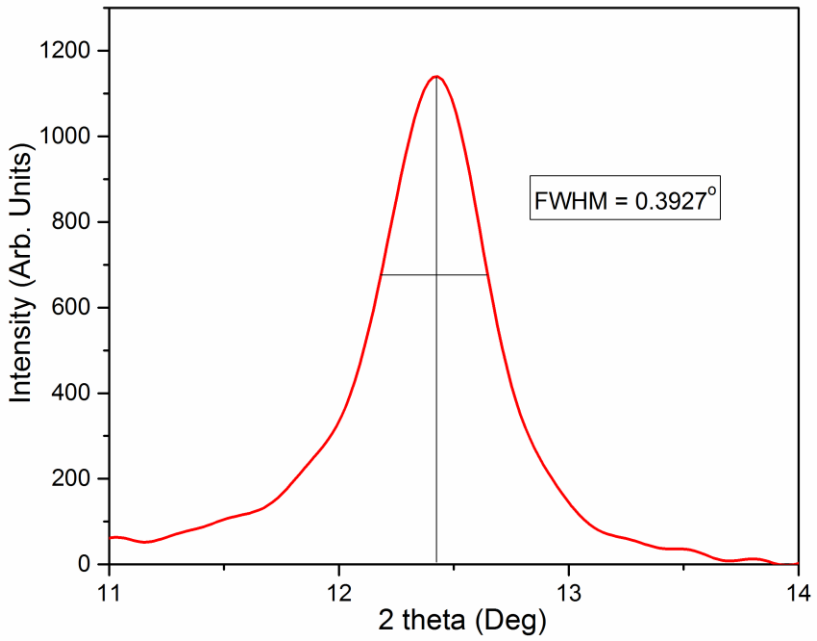

Figure 5.8: Diffraction broadening of Nb_2O_5 thin film at 12.39°

CHAPTER SIX

CONCLUSIONS AND RECOMMENDATIONS

6.1 Conclusions

i. Nb_2O_5 thin films were successfully deposited using the spray pyrolysis technique. The deposition parameters used were as follows: concentration of 0.5 grams per 90ml of solution, a temperature of 270^oC, 370^oC and 470^oC, nozzle to substrate distance of 13 cm and spray duration of 1 minute, 2 minutes and 3 minutes. The films obtained adhered well to the substrates as no peeling effect was observed on the films.

ii. Transmittance of the prepared films was found to range between 60% and 90% and average reflectance was between 10% to 30%. The thickness of the films estimated using the alpha step surface profiler ranged between 162nm and 517nm.

iii. Band gap of the films was estimated to between 3.92 eV to 4.12 eV. No significant differences were observed in band gap values for all the films. Quantum confinement theory explains that semiconductor band gap depends on the size of crystal and its value increases as the crystalline size decreases. Thus the band gap obtained in this work is higher than the previously reported. Sheet resistivity of the prepared Nb_2O_5 thin films is found to range between $10^{-4}\Omega$cm and $10^{-3}\ \Omega$cm.

iv. XRD studies revealed that the films prepared were tetragonal and crystalline in nature. Crystallinity is seen to increase with increase in temperature and spray duration. The average crystalline size is also estimated as approximately 21.27nm.

From the results obtained, the film that was considered as the best for DSSC application is that deposited at 470^{o}C and 2 minutes as they are highly crystalline which means light is likely to be well scattered and also enhance high absorption of the dye. Electrical characteristics indicate that the Nb_2O_5 thin films exhibit semiconductor property. Also transmittance spectra show that the films are transparent within the visible region, which makes them suitable for DSSC application.

6.2 Recommendations

i. The suitability of the thin film in enhancing electron injection into the photoanode and electron transport within the metal oxide semiconductor is usually indicated by the electrical characteristics. In this study, low values of resistivity meant that electrons could flow with ease. However charge carrier density and mobility were not determined and therefore Hall Effect measurements are recommended.

ii. Light harvesting efficiency is one of the key factors that influence light to current conversion efficiency and this is affected by the surface area of the film. In this work, the crystallite size which would influence dye absorption was determined. Hence it is recommendable that surface morphology of the niobium pentoxide thin films to be investigated in order to determine roughness factor as this would affect light scattering.

iii. The fabrication of DSSC solar cell to ascertain the efficiency of the as deposited thin films and also for post annealed films is also recommended.

6.2.1 Recommendation for future studies

i. Investigation of the Effect of precursor concentration on properties niobium pentoxide thin films.

ii. Determination and comparison of DSSC efficiencies prepared using niobium pentoxide photo anodes fabricated by different techniques.

REFERENCES

Aegerter, A., Schimitt, M. and Guo, Y. (2002). Sol-gel niobium pentoxide coatings: Applications to photovoltaic energy conversion and electrochromism. *International Journal of Photoenergy* **4**:1-10

Amita, V. and Singh, V.K. (2013). Sol-gel derived nanostructured niobium pentoxide thin films for electrochromic applications. *Indian Journal of Chemistry* **52A**: 593-598.

Antonio, L.L. (2003). Handbook of Photovoltaic Science and Engineering. 2nd Edition, John Wiley & Sons, Ltd., Hoboken. http://dx.doi.org/10.1002/0470014008

AzoM (2002). Physical vapour deposition – An introduction Retrieved from (https://www.azom.com/article.aspx?ArticleID=1558) 15th November, 2017.

Badawy, W.A. (2015). A Review on Solar Cells from Si-Single Crystals to Porous Materials and Quantum Dots. *Journal of Advanced Research*, **6**: 123-132. Retrieved http://dx.doi.org/10.1016/j.jare.2013.10.001 15th November 2017

Bagher, A.M., Vahid, M.M.A. and Mohsen, M. (2015). Types of Solar Cells and Application. *American Journal of Optics and Photonics*, **3:** 94-113.

Basiru, K. A. and Muhamed, M. (2012). Dye sensitized solar cell using natural dyes extracted from red leave onion. *International Journal of Physical Sciences* **71**:709-712.

Bertolli, M. (2008). Solar Cell Materials. Course: Solid State II. Department of Physics, University of Tennessee,

Bharam V. (2012) Solar Energy: Materials for Photovoltaic Cell. ENGR 232L *Engineering Materials*

Brayner, R. and Bozon-Verduraz, F. (2003). Niobium Pentoxide prepared by soft chemical routes: morphology, structure, defects and quantum size effect. *Physical Chemistry Chemical* **5:**1457-1466,

Çakanyıldırım, M. (2017). Photovoltaic solar energy. Retrieved from https://www.utdallas.edu/~metin/Merit/MyNotes/solarEnergy.pdf 24th June, 2018

Choubey, P.C., Oudhia, A., and Dewangan, R. (2012). A Review: Solar Cell Current Scenario and Future Trends. *Recent Research in Science and Technology*, **4**: 99-101.

Circuit globe (2019). Photovoltaic or Solar Cell retrieved from https://circuitglobe.com/photovoltaic-or-solar-cell.html 25th Jan 2019

Daniel V. S. (1999). An Introduction to Thermal Physics. Pearson; 1 edition (August 28, 1999) ISBN-10: 9780201380279

Donald, S. (2009). Intoduction to solid state chemistry. Massechutes institute of technology. Retrieved from https://ocw.mit.edu/courses/materials-science-and-engineering/3-091sc-introduction-to-solid-state-chemistry-fall-2010/syllabus/MIT3_091SCF09_aln05.pdf 11th June, 2017,

Essner, J. (2011). Dye sensitized optimization of gratzel solar cells towards plasmonic enhanced photovoltaics . *Msc Thesis,* Kansas State university; Kansas.

Friedberg, P. (2002). Four point probe manual. Retrieved from http://wwwinst.eecs.berkeley.edu/~ee143/fa10/lab/four_point_probe.pdf 25th Oct 2013

Ganesh, B.N.V.S. and Supriya, Y.V. (2013). Recent Advancements and Techniques in Manufacture of Solar Cells: Organic Solar Cells. *International Journal of Electronics and Computer Science Engineering*, **2**, 565-573.

Graça M.P.F., Saraiva M., Freire F.N.A., Valente M.A. and Costa L.C. (2015) Electrical analysis of niobium oxide thin films. *An Article in Thin Solid Films* 585 (2015) 95–99

Grein Energy, (2015). Types of Solar Panels, Published 22 April 2015.

Hong-yan C., Dai-bin K. and Cheng-yong S. (2012).Working principles of dye sensitized solar cells. *Journal of Materials Chemistry* **22**:15475-15489

Hoppe, H. and Sariciftci, N.S. (2008). Polymer Solar Cells. *Advances in Polymer Science*, **214**: 4899-4906.

Isrihetty S., Nafarizal N. and Hashim S. (2010) Structural and Electrical Properties of TiO2 Thin Film Derived from Sol-gel Method using Titanium (IV) Butoxide. *International Journal of Integrated Engineering* **2**: 3(2010)

Jacob, S. (2009). "Thin Film Integrated Capacitors with Sputtered-Anodized Niobium Pentoxide Dielectric for Decoupling Applications" *Theses and Dissertations*. 193. Retrieved from http://scholarworks.uark.edu/cgi/viewcontent.cgi?article=1192&context=etd 1st October, 2017

Jasim, K. (2011). Dye sensitized solar cell -working principles, challeges and oppotunities.*Solar cells- dye sensitized devices*, Prof. Leonid A. Kosyachenko (ED), ISBN 798-953-307-735-2, In tech.

Joo-Hee Jang, Tae-Yoo Kim, Nam-Jeong Kim, Chang-Hyoung Lee, Eun-MiPark,Chan Park, and Su-Jeong Suh (2011). Preparation and characterization of Nb_2O_5–Al_2O_3 composite oxide formed by cathodic electroplating and anodizing. *Materials Science and Engineering:* **176**: 1505-1508.

Jung-Ruey T., Neng-fu S. and Rong-Hwei Y. (2015). Effect of deposition temperature on the structural , optical and electrical properties of hydrogenated Ga-doped ZnO film. Retrieved from https://ieeexplore.ieee.org. 3rd Jan 2018.

Kangho K., Nguyen H.D., Mho S. and Lee J. (2013). Enhanced Efficiency of GaAs Single-Junction Solar Cells with Inverted-Cone-Shaped Nanoholes Fabricated Using Anodic Aluminum Oxide Masks. *International Journal of Photoenergy* Volume 2013, Article ID 539765, 5 pages
http://dx.doi.org/10.1155/2013/539765

Kovendhan, M., Joseph, D., Manimuthu P., Ganesan, S., Sambasivan, S. and Maruthamuthu, P. (2011). Spray deposited niobium thin film electrodes for fabrication of dssc. *Transaction of the Indian Institute of Metals* **64**: 185-188.

Krunks, M., Bijakina, O., Mikli, V., Rebane, H., Varema, T., Altosaar, M. and Mellikov, E. (2001). Sprayed CuInS2 thin films for solar cells: The effect of solution composition and post-deposition treatments*Solar Energy Materials and Solar Cells* **69**: 93-98.

Kun-Neng C., Chao-Ming H., Jing L., Yu-Chen L. and Cheng-Fu Y. (2016) Investigation of Antireflection Nb_2O_5 Thin Films by the Sputtering Method under Different Deposition Parameters. *Micromachines* **2016**, 7, 151; doi:10.3390/mi7090151

Lee, J., Rahman, M., Sarker, S., Nath, N. D., Amhammad, A. and Lee, J. K. (2011). Metal oxides and their composites for the photo electrode of dye sensitized solar cell . *Advances in composite materials for medicine and nanotechnology* Dr. Brahim Attaf(ed.)ISNB:978-953-307-235-7,intech ,380-701.

LeViet, A., Jose, M.V., Reddy, B.V.R., Chowdari and Ramakrishna S. (2010). Nb_2O_5 Photoelectrodes for Dye-Sensitized Solar Cells: Choice of the Polymorph. *journal of physics and chemistry* , 114(49) 21795-21800.

Li, B., Wang, L., Kang, B., Wang, P. and Qiu, Y. (2006). Review of Recent Progress in
Solid-State Dye-Sensitized Solar Cells. *Solar Energy Materials and Solar Cells*, **90**: 549-573.

Maehlum, M.A. (2015) Energy Informative The Homeowner's Guide To Solar Panels, Best Thin Film Solar Panels— Amorphous, Cadmium Telluride or CIGS? Last updated 6 April 2015.

Markus Niederberger and Pinna, N. (2009). *Metal Oxide Nanoparticles in Organic Solvents*, Springer London, ch. 2, pp. 7-18.

Mathias M. (2013). Which solar panel is the best? Monocrystalline vs. polycrystalline vs. thin films. Retrieved from http://energyinformative.org/best-solar-panel-monocrystalline-polycrystalline-thin-film/ 5th August 2017

Michael W., Antony P., Rani, R. A., Zoofakar, A. S., O'mullane, and Kourosh, K. Z. (2014). Thin films and nanostructures of niobium pentoxide: fundamental properties , synthesis methods and applications. *journal of materials chemistry* , 2(38) pp. 15683-15703.

Mujawar S.H., Inamdar, A.I. and Patil, S.B. (2006). Electrochromic properties of spray deposited niobium oxide thin films. *Solid State Ionics* **177**: 3333-3338.

Mukrimin S.G. (2016). Solar Power and Appplication Methods. *Renewable and Sustainable Energy Reviews* **57**(2016) 776-785

Naofumi, U., Takuji, K., Fumihiko, M., Yong, J. and Kazuyuki, K. (2003). Low temperature synthesis of niobium oxide nanoparticles from peroxo niobic sol. *Journal of colloid and interface science* **264:** 378-384.

Patil P., Patil A., Mujawar S.H. and Sadale, S.B. (2005). Properties of spray deposited niobium oxide thin films.*Journal of material science ;materials in electronics **16***: 35-41.

Patil, P.S. (1999). Versatility of chemical spray pyrolysis technique. *Materials Chemistry and Physics* **59**: 185-198.

Perednis D. and Gauckler J. (2005). Thin film deposition using spray pyrolysis. *Journal of electroceramics* **14**: 103-111.

Physics and materials science research unit (2017) Electro-deposition. Retrieved from https://wwwfr.uni.lu/recherche/fstc/physics_and_materials_science_research_unit/research_areas/photovoltaics/research/electrodeposition 2nd January 2018

Pierre, A. (1998), in *Introduction to Sol-Gel Processing*, Springer US, vol. 1, ch. 1, pp. 1-9.

Raba M., Bautista-Ruíz J. and Joya M.R. (2016). Synthesis and Structural Properties of Niobium Pentoxide Powders: A Comparative Study of the Growth Process. *Materials Research*, **19**:6 DOI: http://dx.doi.org/10.1590/1980-5373-MR-2015-0733

Rani, Abdul, R., Zoolfakar, A.S., Subbiah; , J.,Ou; , J.Z. and Kalantar -zadeh, K. (2014) Highly ordered anodised Nb_2O_5 nanochannels for dye- sensitized solar cellls. *Electrochemistry Communications* , **40:** 20-13.

Saga, T. (2010). Advances in Crystalline Silicon Solar Cell Technology for Industrial Mass Production. *NPG Asia Materials*, **2**, 96-102. http://dx.doi.org/10.1038/asiamat.2010.82

Sanchez, C., Griesmar P., Papin, G. and Livage, J. (1991). Solgel route to niobium pentoxide. *chemistry of materials* , 335-339.

Sandeep S. and Dhananjaya K. (2015). Effect of Annealing Temperature on the Structural and Optical Properties of Zinc Oxide (ZnO) Thin Films Prepared by Spin Coating Process. *Materials Science and Engineering*, **73:** 012149

Sharma, S., Jain, K. K. and Sharma, A. A. (2015). solar cells in research and applications. *Materials Science and Applications* , **6:** 1145-1155.

Shevgaonkar, R. (2012). *nptel*. Retrieved from nptel.ac.in: http://nptel.ac.in/courses/117101002/downloads/Lec12.pdf 29th December 2017.

Sokolsky, M., & Cirak, J. dye sensitized solar cells :materials and processes. *Acta Electrotenica et informatica* , **10:** 78-81.

Solar energy technologies office (2017). Cadmium-telluride. An office of U.S department of energy. Retrieved from https://www.energy.gov/eere/solar/cadmium-telluride 1st August 2017.

Srinivas, B., Balaji, S., Nagendra Babu, M. and Reddy, Y.S. (2015) Review on Present and Advance Materials for Solar Cells. *International Journal of Engineering Research-Online*, **3**, 178-182.

Thomas Z. (2018). Photovoltaic cell types. Retrieved from http://www.labri.fr/perso/billaud/Helios2/resources/en06/Chapter_6_UB_zimmer.pdf 1st July 2018

Toivola, M. (2010). Dye- sensitized solar cells on alternative substrates. *Doctorial dessertation.* School of science and technology; Aalto University, Finland

Vajpeyi, D. A. (2010). Direct and indirect band gap semiconductors *indian instute of technology Guwahati india* . Retrieved from http://www.iitg.ac.in/: http://www.iitg.ernet.in/eee/ 21st August 2017

Wang, Q., Ito, S., Gratzel, M., Fabregat-Santigo, F., Mora-Sero, I., and Bisquert, J. (2006). characteristic of high efficiency dye sensitized solar cell. *Journal of physical chemistry* **53**:25210-25221.

APPENDIXES

Crystal phase identification of Nb_2O_5 thin film using match software

Sample Data

File name	S1Bib.txt
File path	C:/Users/Godwin A/Desktop/miriam uv
Data collected	Jan 29, 2017 09:40:49
Data range	2.042° - 44.807°
Number of points	2139
Step size	0.020
Rietveld refinement converged	No
Alpha2 subtracted	Yes
Background subtr.	Yes
Data smoothed	Yes
Specimen displacement correction (Bragg-Brentano geometry)	T = (-s/R) = 0.00056
Radiation	X-rays
Wavelength	1.540598 Å

Matched Phases

Index	*Amount (%)*	*Name*	*Formula sum*
A	100.0	Nb2 O5	Nb2 O5
	42.8	*Unidentified peak area*	

A: Nb2 O5 (100.0 %)

Formula sum	Nb2 O5
Entry number	96-152-8724
Figure-of-Merit (FoM)	0.478150
Total number of peaks	237
Peaks in range	39
Peaks matched	13
Intensity scale factor	1.96
Space group	I 4/m m m
Crystal system	tetragonal
Unit cell	a= 20.4400 Å c= 3.8320 Å
I/Ic	5.30
Calc. density	4.410 g/cm³
Reference	Martin W., Gruehn R., Andersson S., "Ueber die Kristallstruktur von M - Nb2 O5", Journal of Solid State Chemistry **1**, 419-424 (1970)

Candidates

Name	*Formula*	*Entry No.*	*FoM*
Nb2 O5	Nb2 O5	96-152-8724	0.4754
Nb2 O5	Nb2 O5	96-153-4157	0.4479
Nb12 O29	Nb12 O29	96-412-3974	0.4384
Nb12 O29	Nb12 O29	96-154-1319	0.4116
Nb2 O5	Nb2 O5	96-210-7338	0.3027
Nb2 O5	Nb2 O5	96-231-0582	0.2682
Nb4 O5	Nb4 O5	96-153-4620	0.2151
	Nb O2	96-900-9094	0.1964
Nb O2	Nb O2	96-152-0792	0.1916
Nb O2	Nb O2	96-153-8349	0.1902
Nb O2	Nb O2	96-153-8350	0.1901
Nb O2	Nb O2	96-210-6755	0.1901
Nb O2	Nb O2	96-154-2079	0.1821
Nb2 O5	Nb2 O5	96-152-8679	0.1817
	Nb2 O7	96-721-2096	0.1790
Nb16.8 O42	Nb16.8 O42	96-210-6535	0.1444
Niobium(II) oxide	Nb O	96-101-0411	0.0000
Nb O.76	Nb O0.76	96-153-0155	0.0000
Nb O	Nb O	96-153-1803	0.0000
	Nb O	96-900-8685	0.0000
	Nb O	96-900-8783	0.0000
	Nb O3	96-901-5166	0.0000

Search-Match

Settings

Reference database used	COD-Inorg REV184238 2016.07.05
Automatic zeropoint adaptation	Yes
Minimum figure-of-merit (FoM)	0.60
2theta window for peak corr.	0.30 deg.
Minimum rel. int. for peak corr.	1
Parameter/influence 2theta	0.50
Parameter/influence intensities	0.50
Parameter multiple/single phase(s)	0.50

Selection Criteria

Elements:

Elements that must be present:	O, Nb
Elements that must NOT be present:	All elements not mentioned above

Criteria for entries added by user

X RD pattern of Nb_2O_5 thin film obtained using match software.